

NASA Contractor Report 4397

IN-35

51125

P-64

Attitude Identification
for SCOLE Using
Two Infrared Cameras

Joram Shenhar

CONTRACT NAS1-19000
OCTOBER 1991

(NASA-CR-4397) ATTITUDE IDENTIFICATION FOR
SCOLE USING TWO INFRARED CAMERAS Interim
Report (Lockheed Engineering and Sciences
Corp.) 64 p

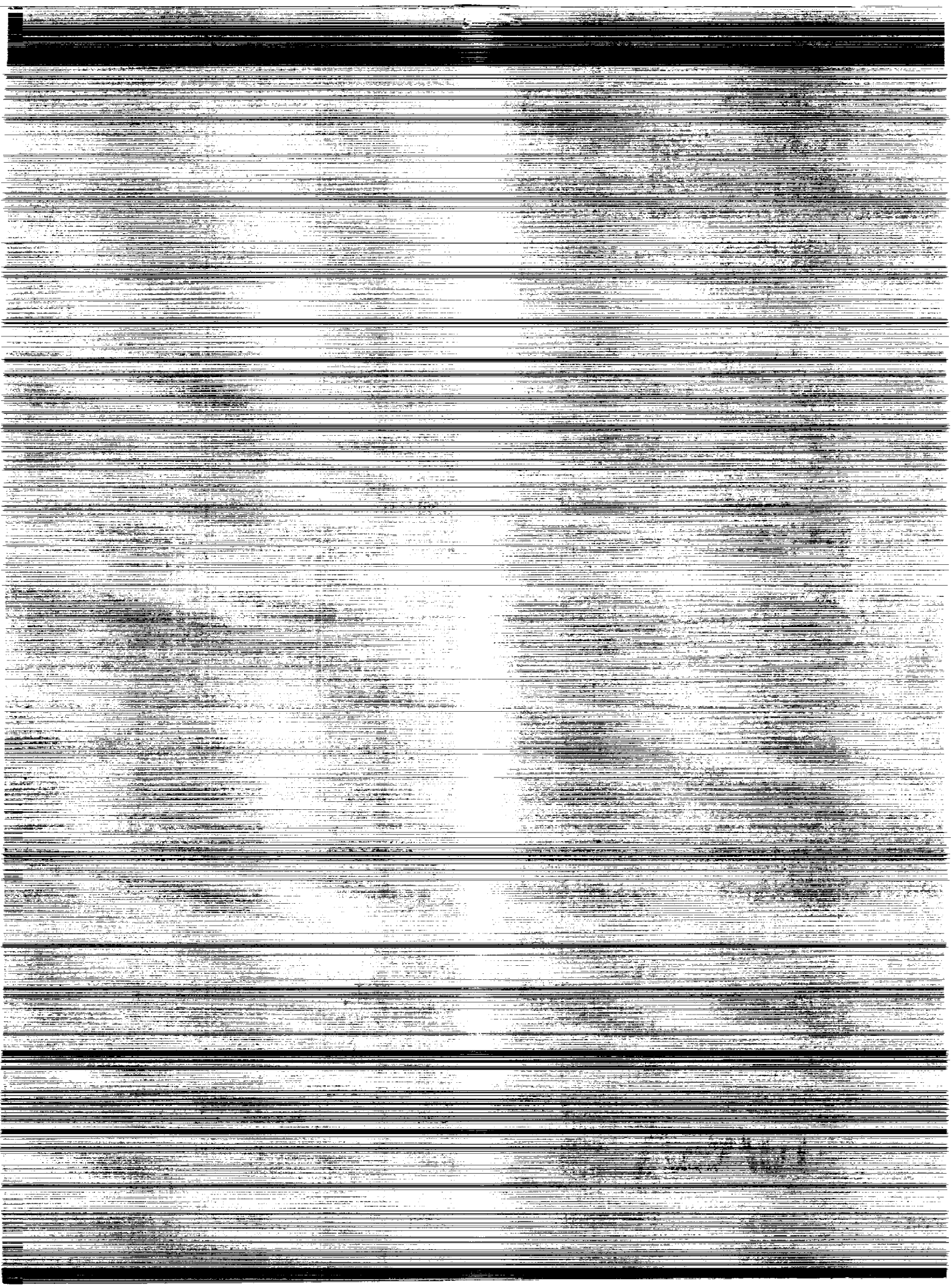
CSCL 14E

N92-11338

Unclas
0051125

H1/35

NASA



NASA Contractor Report 4397

Attitude Identification for SCOLE Using Two Infrared Cameras

Joram Shenhar
Lockheed Engineering & Sciences Company
Hampton, Virginia

Prepared for
Langley Research Center
under Contract NAS1-19000



National Aeronautics and
Space Administration

Office of Management

Scientific and Technical
Information Program

1991

~~SECRET~~ INTENTIONALLY BLANK

TABLE OF CONTENTS

ABSTRACT.....	iv
LIST OF TABLES.....	v
LIST OF FIGURES.....	vi
LIST OF SIMBOLS.....	vii
I. INTRODUCTION.....	1
II. THE TESTING SYSTEM.....	3
III. A SUMMARY OF ESSENTIAL TRANSFORMATION EQUATIONS.....	5
IV. CAMERA PLACEMENT IDENTIFICATION.....	8
V. SCOLE ATTITUDE TRACKING.....	11
VI. NUMERICAL RESULTS AND DISCUSSION.....	15
VII. CONCLUDING REMARKS.....	18
VIII. REFERENCES.....	20
APPENDIX	
PC-MATLAB COMPUTER CODE FOR CAMERA PLACEMENT	
IDENTIFICATION AND SCOLE ATTITUDE TRACKING.....	42

ABSTRACT

This report presents an algorithm that incorporates real-time data from two infrared cameras and computes the attitude parameters of the Spacecraft COntrol Laboratory Experiment (SCOLE), a laboratory apparatus representing an offset-feed antenna attached to the Space Shuttle by a flexible mast. The algorithm utilizes camera position information of three miniature light emitting diodes (LEDs), mounted on the SCOLE platform, permitting arbitrary camera placement and an on-line attitude extraction. The continuous nature of the algorithm allows identification of the placement of the two cameras with respect to some initial position of the three reference LEDs, followed by on-line six degrees of freedom attitude tracking, regardless of the attitude time history. The report provides a description of the algorithm in the camera identification mode as well as the mode of target tracking. Experimental data from a reduced-size SCOLE-like laboratory model, reflecting the performance of the camera identification and the tracking processes, are presented. Computer code for camera placement identification and SCOLE attitude tracking is listed.

LIST OF TABLES

I.- Cameras orientation angles α , β , and ϵ and scale factors λ	23
--	----

LIST OF FIGURES

1.-	The Spacecraft Control Laboratory Experiment - SCOLE.....	24
2.-	SCOLE laboratory upper level view with two camera towers.....	25
3.-	Laboratory setup of infrared detector cameras and the SCOLE reduced-size model.....	26
4.-	SCOLE reduced-size model with LED configuration.....	27
5.-	Camera placement angles in Newtonian coordinates system.....	28
6.-	True position (y,z) of a light spot on detector plane.....	29
7.-	Coordinate system transformation.....	30
8.-	LED placement configuration on SCOLE.....	31
9.-	LED image location and origin determination geometry on detector plane.....	32
10.-	LED triangular configuration on SCOLE.....	33
11.-	A typical solution to Eq.(5): polynomial first root ϵ_0	34
12.-	SCOLE attitude angle extraction.....	35
13.-	A typical scaled-image in the camera placement mode.....	36
14.-	Camera scaled-image at various model orientations.....	37
15.-	Yaw, pitch, and roll measurements versus rotary stage position.....	38
16.-	Yaw attitude error via linear least-squares approximation.....	39
17.-	Camera scaled view of center-of-mass motion.....	40
18.-	$x^{(0)}, y^{(0)}, z^{(0)}$ components of center-of-mass motion.....	41

LIST OF SIMBOLS

A, B, C	constant coefficients
A	least-squares approximation matrix
b, h, l	SCOLE LEDs placement measurements
b	least-squares approximation constant vector
dist(k,l)	distance between points k and l
ell	least-squares approximation error parameter
F	function symbol
R, R _i , R*	three-rotations global transformation matrices
R _{ij}	ijth entry of matrix R
v ^(j)	3x1 Newtonian coordinate vector of point j
v ⁽⁰⁾	3x1 Newtonian coordinate vector of center of mass
v _i ^(j)	3x1 coordinate vector of point j in the ith frame
v _i ^(j0)	3x1 relative measurements vector of point j with respect to the computed origin 0 in camera frame
x, y, z	Newtonian frame
x ⁽⁰⁾ , y ⁽⁰⁾ , z ⁽⁰⁾	Newtonian frame absolute displacements of center of mass
x _i , y _i , z _i	coordinate sets: i=0 parallel translation to Newtonian frame i=1 first rotation about z ₀ i=2 second rotation about y ₁ i=c third rotation about x ₂ - camera body frame i=s SCOLE model body frame

x	least-squares approximation vector of unknowns
y, z	image coordinates on detector plane
α, β, ϵ	camera yaw, pitch and roll angles
ψ, ϑ, ϕ	SCOLE yaw, pitch and roll angles
$[\alpha], [\beta], [\epsilon]$	single-rotation transformation matrices
λ	camera scale factor
dist	distance
LED	light emitting diode
LS	least squares
SCOLE	Spacecraft Control Laboratory Experiment
sgn	the standard sign function

I. INTRODUCTION

The development of control laws for flexible structures has received considerable attention. To support research in this area, the NASA Langley Research Center has developed the Spacecraft Control Laboratory Experiment (SCOLE) (refs. 1-2). This facility provides researchers with a highly flexible test article, sensors, actuators, and digital control processing capability. The test article mimics the Space Shuttle with a large, flexible, offset-feed antenna attached to the payload bay as shown in figure 1. Much interest has been expressed by the research community concerning SCOLE. This is reflected in the technical output of five workshops conducted by the NASA Langley Research Center (refs. 3-7). Using SCOLE, control laws for a multi-input/multi-output structural dynamics system can be implemented in real time from any remote site that has a computer terminal and an asynchronous serial communications capability. Recent real-time experiments, representing a wide variety of applications related to dynamics and control of flexible structures, revealed good agreement with simulation results (refs. 8-9).

Two main control objectives are stated for SCOLE (ref. 1). The first is a minimum-time slew through a large angle (20 degrees) reorienting and maintaining the "Shuttle" platform attitude to within a prescribed offset from an arbitrary line-of-sight reference. The second is a rotation of 90 degrees about the line-of-sight while preparing for another slew maneuver. Two research and design stages are presented

by the SCOLE challenge. The first deals with the development of control laws for a mathematical model of the structure in Earth orbit, while the second is the design and implementation of the control laws on a laboratory representation of the structural dynamics system. This report supports, in part, the second stage of the design challenge by presenting an algorithm to accommodate rigid-body motion tracking. To detect slew maneuver and rotation about the line-of-sight, it is proposed to utilize the capabilities of an infrared detector system comprised of two cameras and three light emitting diodes (LEDs). Figure 2 shows the laboratory upper level with the two camera towers and the SCOLE LED target system. The use of such a non-inertial sensing device reduces the complexity inherent in any inertial sensor system and provides direct displacement measurements. In this report, a description of the test system and the algorithm for the camera self-calibration mode and target tracking mode are provided. Experimental data and test results from a reduced-size SCOLE-like laboratory model, shown in figures 3 and 4, are presented. The results reflect the performance of the camera identification and tracking processes.

II. THE TEST SYSTEM

A detailed description of the SCOLE hardware and support software is provided in (ref. 2). It proved convenient to develop and test the proposed infrared detector system for SCOLE attitude extraction in a separate optics laboratory. To this end, a reduced size SCOLE-like model was designed. Figure 3 shows the model, mounted to a computer-controlled single degree-of-freedom precision rotary stage, as well as the infrared detector cameras. This setup provides a reduced dimension testbed that simulates the actual configuration of the SCOLE system, shown in figure 2. The three external LEDs, shown in figure 4, used in the experiment, resemble the isosceles-triangle SCOLE-LED configuration. This particular LED placement reduces the complexity of the nonlinear, rigid-body, transformation equations, permitting closed-form solution for attitude determination.

Two infrared cameras were arbitrarily positioned to detect the three LED images during the maneuver of the SCOLE model, as shown in figure 5. The camera lens assembly focuses any light source within its field of view onto a special photodiode. The two-axis "lateral effect photodiode" has four electrodes on its edges. When a light spot is imaged onto its surface, electric current is generated, divided up among the four electrodes in proportion to the distance of the light spot from these electrodes. Denoting the detector outputs as y_1 , y_2 , z_1 , and z_2 , for the positive y, negative y, positive z, and negative z, respectively, one can determine the normalized (y,z) coordinates of the image spot on

the detector plane, as described in figure 6, using the following expressions (ref. 10):

$$y = \frac{y_1 - y_2}{y_1 + y_2}, \quad z = \frac{z_1 - z_2}{z_1 + z_2}$$

The resulting algebraic quantities are independent of the light intensity. Both cameras are interfaced to a PC-AT computer, which processes the sensor information and computes the rigid-body attitude angles and translation displacement of the SCOLE model center of mass.

III. A SUMMARY OF ESSENTIAL TRANSFORMATION EQUATIONS

Assuming that light rays travel in straight lines, enter a distortionless camera lens system through a single point, then a projective relationship exists between the photographic coordinates of the image points and the ground coordinates of the corresponding object points, as illustrated in figure 7. To describe the orientation of the camera relative to the inertial frame, x, y, z , it suffices to state the orientation of the body-fixed camera coordinates, x_c, y_c, z_c , relative to the SCOLE model reference frame x_0, y_0, z_0 . At this stage, the SCOLE is fixed to the inertial frame such that reference frames x, y, z and x_0, y_0, z_0 coincide. This projective relationship can be accomplished by means of three consecutive rotations. Since the transformation law deals with large rotations, emphasis is placed on "consecutive" rotation because the order in which these rotations are carried out is important.

The following rotations are applied:

1. Coordinate system x_1, y_1, z_1 is rotated about the z_0 axis over an angle α , positive as indicated in figure 7. The angle α is referred to as the heading or yaw angle.
2. Coordinate system x_2, y_2, z_2 is rotated about the y_1 axis over an angle β , positive as indicated in figure 7. The angle β is referred to as the attitude or pitch angle.

3. Coordinate system x_c, y_c, z_c is rotated about the x_2 axis over an angle ϵ , positive as indicated in figure 7. The angle ϵ is referred to as the bank or roll angle.

The angles α, β and ϵ are frequently referred to as Euler angles.

Defining $v_i^{(j)}$ as the 3×1 coordinate vector of point j projected onto coordinate system i , the transformation law that relates the camera frame to the reference frame can be written as

$$v_c^{(j)} = Rv^{(j)} \quad (1)$$

$v^{(j)}$ is the Newtonian coordinate vector of LED j , positioned on the SCOLE model as shown in figure 8. The relative camera measurement vector $v_c^{(j)}$ in equation 1 indicates the coordinates vector of LED j image on the camera's detector plane with respect to the computed camera origin O_c , shown in figure 9.

The ratio between sections along a straight line is known to be invariant under coordinate transformation. This observation facilitates the determination of the origin coordinates in the camera's frame, based on the given triangular geometry that appears in figure 10. The extended lines (1,2) and (0,3) intersect at point M_{12} . Similarly, lines (0,1) and (2,3) intersect at point M_{23} . Since the distance ratios: $\text{dist}(1, M_{12})/\text{dist}(1, 2)$, and $\text{dist}(2, M_{23})/\text{dist}(2, 3)$ are unaltered, camera image coordinates of points M_{12} and M_{23} can be determined, based upon these ratios and camera measurement of LED-image coordinates at points 1, 2, and 3, as shown in figure 9. Coordinates of the intersection

point of lines (3,M₁₂) and extension of (1,M₂₃), constitute the image origin O_c on the detector plane.

The matrix R in equation 1 is the 3x3 transformation matrix, based upon the three consecutive rotations α, β, and ε

$$[\alpha] = \begin{bmatrix} c\alpha & s\alpha & 0 \\ -s\alpha & c\alpha & 0 \\ 0 & 0 & 1 \end{bmatrix} \quad [\beta] = \begin{bmatrix} c\beta & 0 & -s\beta \\ 0 & 1 & 0 \\ s\beta & 0 & c\beta \end{bmatrix} \quad [\epsilon] = \begin{bmatrix} 1 & 0 & 0 \\ 0 & c\epsilon & s\epsilon \\ 0 & -s\epsilon & c\epsilon \end{bmatrix}$$

where the notations "s" and "c" abbreviate the trigonometric functions "sin" and "cos", respectively. In particular, the global transformation matrix can be expressed as

$$R = [\epsilon][\beta][\alpha] = \begin{bmatrix} R_{11} & R_{12} & R_{13} \\ R_{21} & R_{22} & R_{23} \\ R_{31} & R_{32} & R_{33} \end{bmatrix} \quad (2a)$$

where

$$\begin{aligned} R_{11} &= \cos(\beta)\cos(\alpha) \\ R_{12} &= \cos(\beta)\sin(\alpha) \\ R_{13} &= -\sin(\beta) \\ R_{21} &= -\cos(\epsilon)\sin(\alpha) + \sin(\epsilon)\sin(\beta)\cos(\alpha) \\ R_{22} &= \cos(\epsilon)\cos(\alpha) + \sin(\epsilon)\sin(\beta)\sin(\alpha) \\ R_{23} &= \sin(\epsilon)\cos(\beta) \\ R_{31} &= \sin(\epsilon)\sin(\alpha) + \cos(\epsilon)\sin(\beta)\cos(\alpha) \\ R_{32} &= -\sin(\epsilon)\cos(\alpha) + \cos(\epsilon)\sin(\beta)\sin(\alpha) \\ R_{33} &= \cos(\epsilon)\cos(\beta) \end{aligned} \quad (2b)$$

IV. CAMERA PLACEMENT IDENTIFICATION

Utilizing the symmetry property of the LED configuration shown in figure 10 and introducing the camera scale factor λ as the unknown ratio between the dimensions of the SCOLE model and the camera image, the following relationships for LEDs 1, 2, and 3 are proper:

$$\begin{aligned} \mathbf{v}^{(1)} &= [\mathbf{l} \ 0 \ 0]^T, & \mathbf{v}_c^{(10)} &= \mathbf{v}_c^{(1)} - \mathbf{v}_c^{(0)} \\ \mathbf{v}_c^{(10)} &= \frac{1}{\lambda} \mathbf{R} \mathbf{v}^{(1)} = \frac{\mathbf{l}}{\lambda} [\mathbf{R}_{11} \ \mathbf{R}_{21} \ \mathbf{R}_{31}]^T \end{aligned} \quad (3a)$$

$$\begin{aligned} \mathbf{v}^{(2)} &= [-h \ 0 \ 0]^T, & \mathbf{v}_c^{(20)} &= \mathbf{v}_c^{(2)} - \mathbf{v}_c^{(0)} \\ \mathbf{v}_c^{(20)} &= \frac{1}{\lambda} \mathbf{R} \mathbf{v}^{(2)} = \frac{1}{\lambda} [-\mathbf{R}_{11}h + \mathbf{R}_{12}b \quad -\mathbf{R}_{21}h + \mathbf{R}_{22}b \quad -\mathbf{R}_{31}h + \mathbf{R}_{32}b]^T \end{aligned} \quad (3b)$$

$$\begin{aligned} \mathbf{v}^{(3)} &= [-h \ -b \ 0]^T, & \mathbf{v}_c^{(30)} &= \mathbf{v}_c^{(3)} - \mathbf{v}_c^{(0)} \\ \mathbf{v}_c^{(30)} &= \frac{1}{\lambda} \mathbf{R} \mathbf{v}^{(3)} = \frac{1}{\lambda} [-\mathbf{R}_{11}h - \mathbf{R}_{12}b \quad -\mathbf{R}_{21}h - \mathbf{R}_{22}b \quad -\mathbf{R}_{31}h - \mathbf{R}_{32}b]^T \end{aligned} \quad (3c)$$

where \mathbf{l} , h , and b are the SCOLE LED placement measurements, as indicated in figure 10. Introducing the relative measurement vector components $\mathbf{v}_c^{(j0)} = [x_c^{(j0)} \ y_c^{(j0)} \ z_c^{(j0)}]^T$ and substituting equations 2b into 3b and 3c, the following expressions can be derived

$$-\cos(\epsilon)\sin(\alpha) + \sin(\epsilon)\sin(\beta)\cos(\alpha) = -\lambda \frac{y_c^{(20)} + y_c^{(30)}}{2h} \quad (4a)$$

$$\sin(\epsilon)\sin(\alpha) + \cos(\epsilon)\sin(\beta)\cos(\alpha) = -\lambda \frac{z_c^{(20)} + z_c^{(30)}}{2h} \quad (4b)$$

$$\cos(\epsilon)\cos(\alpha) + \sin(\epsilon)\sin(\beta)\sin(\alpha) = \lambda \frac{y_c^{(20)} - y_c^{(30)}}{2b} \quad (4c)$$

$$-\sin(\epsilon)\cos(\alpha) + \cos(\epsilon)\sin(\beta)\sin(\alpha) = \lambda \frac{z_c^{(20)} - z_c^{(30)}}{2b} \quad (4d)$$

An explicit expression for ϵ can be obtained by eliminating α and β from equations 4, yielding the (ϵ, λ) polynomial

$$F(\epsilon, \lambda) = A \cos^2(\epsilon) + B \cos(\epsilon)\sin(\epsilon) + C \sin^2(\epsilon) - 1 = 0 \quad (5a)$$

where

$$A = \lambda^2 \left\{ \left(\frac{y_c^{(20)} + y_c^{(30)}}{2h} \right)^2 + \left(\frac{y_c^{(20)} - y_c^{(30)}}{2b} \right)^2 \right\} = R_{21}^2 + R_{22}^2$$

$$B = -\lambda^2 \left\{ \frac{(y_c^{(20)} + y_c^{(30)})(z_c^{(20)} + z_c^{(30)})}{2h^2} + \frac{(y_c^{(20)} - y_c^{(30)})(z_c^{(20)} - z_c^{(30)})}{2b^2} \right\}$$

$$= -2(R_{21}R_{31} + R_{22}R_{32})$$

$$C = \lambda^2 \left\{ \left(\frac{z_c^{(20)} + z_c^{(30)}}{2h} \right)^2 + \left(\frac{z_c^{(20)} - z_c^{(30)}}{2b} \right)^2 \right\} = R_{31}^2 + R_{32}^2 \quad (5b)$$

are constants, based on the SCOLE configuration parameters h , b , camera measurements $y_c^{(j0)}$, $z_c^{(j0)}$, ($j=2,3$), and the unknown camera constant scale factor λ . Substitution of expressions 2b for R_{mn} ($m,n = 1,2,3$) in equations 5b and then in equation 5a, must satisfy the identity $F(\epsilon, \lambda) \equiv 0$. Moreover, differentiating equation 5a with respect to ϵ and

using equations 2b and 5b again, reveals $\partial F(\epsilon, \lambda) / \partial \epsilon \equiv 0$. These observations constitute the method for the determination of the camera roll angle ϵ and scale factor λ . A typical solution to equation 5 is displayed in figure 11. Camera yaw angle α and pitch angle β are obtained from equations 4

$$\alpha = \sin^{-1} [s_1 \cos(\epsilon) - s_2 \sin(\epsilon)] \quad (6)$$

$$\beta = \sin^{-1} \left[\frac{c_2 + \sin(\epsilon) \cos(\alpha)}{\cos(\epsilon) \sin(\alpha)} \right] \quad (7)$$

where

$$s_1 = (y_c^{(20)} + y_c^{(30)}) \left\{ - \operatorname{sgn} [v_0^{(2)}(1)] \right\} / (2h)$$

$$s_2 = (z_c^{(20)} + z_c^{(30)}) \left\{ - \operatorname{sgn} [v_0^{(2)}(1)] \right\} / (2h)$$

$$c_2 = (z_c^{(20)} - z_c^{(30)}) / (2b)$$

$\operatorname{sgn} [v_0^{(2)}(1)]$ is the standard sign function with the first entry of vector $v_0^{(2)}$ from equation 3b as an argument.

The method of determination of the orientation angles α , β , and ϵ , for both cameras described herein, permits arbitrary camera placement. The three-LED system mounted on the initially fixed SCOLE model during this process constitutes the reference Newtonian frame for the attitude tracking mode.

V. SCOLE ATTITUDE TRACKING

The SCOLE tracking process is related to the identification of the three displacement components, $x^{(0)}$, $y^{(0)}$, $z^{(0)}$, of the SCOLE center of mass, and the yaw, pitch, and roll attitude angles ψ , ϑ , ϕ , of its platform, respectively, as shown in figure 12, and can be regarded as the reversed version of the camera placement identification algorithm.

Substitution of the identified camera orientation angles α_i , β_i , and ϵ_i , ($i=1,2$), yields the transformation relations between each camera and the SCOLE model

$$v_{c1}^{(j0)} = R_1 v_0^{(j)}, \quad v_{c2}^{(j0)} = R_2 v_0^{(j)} \quad (8a,b)$$

where

$$v_0^{(j)} = v^{(j)} - v^{(0)} \quad (8c)$$

In these equations R_1 and R_2 are the constant coefficient transformation matrices in the form of equation 2, evaluated for camera 1 and 2 angles α_1 , β_1 , ϵ_1 , and α_2 , β_2 , ϵ_2 , respectively. In a similar manner $v_{c1}^{(j0)}$ and $v_{c2}^{(j0)}$ indicate the relative coordinate vector of LED j image onto camera 1 and 2 body frame with respect to the instantaneous computed image of the SCOLE model origin 0. $v^{(j)}$ and $v^{(0)}$ in equation 8c are the Newtonian coordinate vector of LED j and the SCOLE model origin 0, respectively. $v_0^{(j)}$ is the LED j coordinate vector in the translated frame x_0, y_0, z_0 . Eliminating $v_0^{(j)}$ from

equations 8a,b, yields the transformation relation between the two cameras

$$v_{c1}^{(j0)} = R^* v_{c2}^{(j0)}, \quad R^* = R_1 R_2^{-1}, \quad j = 0,1,2,3 \quad (9)$$

$j=0$ represents the displacement of the image instantaneous center of mass with respect to the computed image fixed origin. Expressing $v_{ci}^{(j0)}$ ($i=1,2$) in terms of the Cartesian components $v_{c1}^{(j0)} = [x_{c1}^{(j0)} \ y_{c1}^{(j0)} \ z_{c1}^{(j0)}]^T$, and $v_{c2}^{(j0)} = [x_{c2}^{(j0)} \ y_{c2}^{(j0)} \ z_{c2}^{(j0)}]^T$, an explicit expression for $x_{c1}^{(j0)}$ and $x_{c2}^{(j0)}$ can be derived

$$A x_j = b_j, \quad j = 0,1,2,3 \quad (10)$$

where

$$A = \begin{bmatrix} 1 & -R_{11}^* \\ 0 & -R_{21}^* \\ 0 & -R_{31}^* \end{bmatrix}, \quad x_j = [x_{c1}^{(j0)} \ x_{c2}^{(j0)}]^T, \quad b_j = \begin{bmatrix} R_{12}^* & R_{13}^* \\ R_{22}^* & R_{23}^* \\ R_{32}^* & R_{33}^* \end{bmatrix} \begin{Bmatrix} y_{c2}^{(j0)} \\ z_{c2}^{(j0)} \end{Bmatrix} - \begin{Bmatrix} 0 \\ y_{c1}^{(j0)} \\ z_{c1}^{(j0)} \end{Bmatrix}$$

Because this set of three equations contains only two unknown quantities, $x_{c1}^{(j0)}$ and $x_{c2}^{(j0)}$, it is said to be overdetermined and any subset of two equations may, in principle, be solved to recover $x_{c1}^{(j0)}$ and $x_{c2}^{(j0)}$. In practice, however, the detector plane image coordinates $y_{ci}^{(j0)}$, $z_{ci}^{(j0)}$ are known within some error bound. Consequently, solutions to the various subsets of two equations will yield somewhat different results. In such a case, a preferable practice is to employ the method of Least Squares (LS) to extract from the entire set of three

equations a reduced set of two equations leading to results of greatest possible accuracy. Using standard LS approximation, the recovered unknown vectors x_j are obtained by

$$x_j = (A^T A)^{-1} A^T b_j, \quad j = 0,1,2,3 \quad (11)$$

and the amount of error in this approximate solution is indicated by

$$\|e\|_j^2 = b_j^T [I - A(A^T A)^{-1} A^T] b_j \quad (12)$$

With the recovered x_j vectors, the camera information is complete and available for the determination of the global coordinates of the three SCOPE LEDs. This can be accomplished by using the inverse transformation

$$\begin{bmatrix} x_0^{(j)} & y_0^{(j)} & z_0^{(j)} \end{bmatrix}^T = R_i^{-1} \begin{bmatrix} x_{ci}^{(j0)} & y_{ci}^{(j0)} & z_{ci}^{(j0)} \end{bmatrix}, \text{ for } i=1 \text{ or } i=2, j=1,2,3 \quad (13)$$

Subsequently, the angular motion parameters, ψ , ϑ , and ϕ are calculated, based on the above information and the geometry of figure 12:

$$\psi = \tan^{-1} \frac{y_0^{(1)}}{x_0^{(1)}} \quad (14)$$

$$\vartheta = \tan^{-1} \left[\frac{z_0^{(1)}}{\sqrt{(x_0^{(1)})^2 + (y_0^{(1)})^2}} \right] \quad (15)$$

$$\phi = \sin^{-1} \left[\frac{z_0^{(2)} + h \operatorname{sgn} [v_0^{(2)}(1)] \sin(\vartheta)}{b \cos(\vartheta)} \right] \quad (16)$$

where superscripts in equations 14 through 16 indicate LED index number and the subscripts are associated with the related coordinate system. Similarly, the displacement vector of the SCOLE center of mass is obtained by the inverse transformation

$$[x^{(0)} \ y^{(0)} \ z^{(0)}]^T = R_i^{-1} [x_{ci}^{(00)} \ y_{ci}^{(00)} \ z_{ci}^{(00)}], \text{ for } i=1 \text{ or } i=2 \quad (17)$$

where $x^{(0)}, y^{(0)}, z^{(0)}$, are absolute displacement components of the SCOLE center of mass and $x_{ci}^{(00)}, y_{ci}^{(00)}, z_{ci}^{(00)}$, represent the camera frame displacement of the instantaneous center-of-mass image with respect to the camera-fixed origin.

The continuous nature of the algorithm permits instantaneous tracking of the SCOLE attitude regardless of the trajectories time history. Using tracking techniques based on classical methods (ref. 11), current attitude estimate depends on the preceding estimate. With this approach, in a case when the target signal is temporarily lost or corrupted during operation, it will be most difficult, if not impossible, to relocate the model without process interruption.

VI. NUMERICAL RESULTS AND DISCUSSION

Rigid body attitude maneuver tracking was tested on a reduced-size SCOLE-like laboratory model using the methods and equipment previously described. For this work, due to hardware limitations, the model was attached at its center of mass to a single degree-of-freedom, precision, rotary stage, as shown in figure 4, resulting in rotation about the yaw axis only. The rotary stage controller was able to provide motion with a resolution of 0.001 degrees. This laboratory setup provides a dynamics-free environment, where the sole testing of software and sensor hardware is performed. The experiment consists of two phases. During phase I, both cameras were oriented such that all of the light sources appear within the field of view of each camera, but otherwise arbitrarily. The SCOLE model was oriented to a desired initial position where the SCOLE body frame at that instant constitutes the system inertial reference. Camera identification, based upon the procedure previously described, yields camera orientation angles with respect to Newtonian frame, as well as camera scale factors. Sensor measurements, summarized in Table I, are consistent with results based on external measurement. Figure 13 displays a typical scaled LED image on the detector plane in the camera identification mode.

Phase II of the experiment deals with attitude tracking of the SCOLE model. During this phase, the rotary stage was turned and LED position measurements were detected by both cameras simultaneously at every 5-degree increment. Figure 14 displays camera scaled images

at various model orientations. Figure 15 depicts sensor outputs for a rotation range of 50 degrees, where each measurement is based on the average of six samples. Due to the system constraints, yaw was the only attitude change expected. However, as shown in figure 15, non-zero pitch and roll motion were detected as well. This is due to misalignment between the LED-plane normal vector and the rotary stage axis of rotation. The same offset also affects the yaw measurements resulting in deviation from the expected linear characteristics. Defining linearity error as the difference between a data point and the associated linear least-squares approximation of the entire data set, the average error over the range of 50 degrees was 0.56 degrees. Figure 16 displays the yaw error characteristics, spanned over the experimental range. Although motion of the model center of mass was constrained by the experimental setup, non-zero displacement components were detected by both cameras, as shown in figures 17 and 18. The first figure exhibits a camera scaled view of the image center-of-mass motion while the second provides a description of the motion components in an Newtonian frame. These unexpected readings are due primarily to detector non-linearities.

Error reduction can be achieved through system upgrading. This amounts to sensor random-noise level reduction by replacement of the existing LEDs with more powerful ones along with amplifier gain reduction. Uncertainties in measurements of the LED configuration on the SCOLE model, and possible offset between the location of the camera image computed origin and the axis of rotation of the rotary stage, contribute to error accumulation. Another error source is encountered

with sensor distortion. Because of geometrical considerations involving detector electrode placement, the most linear region of the detector is the 25-percent zone around its center. However, for maximum linearity, the center 6.25-percent zone of the detector should be used (ref. 10). Minimum linearity zone is observed at the corner of the detector; however, as the image spot moves towards the center, linearity is improved. Applications needing the maximum accuracy require distortion mapping of the detector surface and lens calibration. Such procedures were presented in (ref. 12), where a distortion correction was determined by fitting the sensor data to scanner data, using least-squares approximation. Correction of misalignment associated with the scanning operations and a table lookup procedure to map the detector surface can improve image distortion correction, and, therefore, increase camera output accuracy.

VII. CONCLUDING REMARKS

An attitude tracking algorithm, utilizing position information of three selected fixed points on the SCOLE platform, was introduced. The data acquisition system utilizes the capabilities of an infrared detector system comprised of two cameras, fixed to a Newtonian frame, and three light emitting diodes, attached to three selected points on SCOLE. Both cameras are interfaced to a PC-AT computer which processes sensor information and computes the SCOLE rigid-body attitude angles and displacement vector of its center of mass. The experiment consists of two phases. During phase I, both cameras are operating in the self-calibration mode, where orientation angles for each camera body frame with respect to the Newtonian frame are determined. In addition, the scale factor for each camera, defined as the ratio between the physical dimensions of the object and its image on the detector surface, is computed. During phase II, both cameras are operating in the tracking mode, where position information of the three LEDs is acquired and instantaneous yaw, pitch, and roll angles, as well as centroid displacement components, are determined. Yaw maneuver tests, performed on a reduced-size SCOLE-like laboratory model, revealed an average linearity error of 0.56 degrees over the range of 50 degrees. The results obtained here agree with other results obtained when a nonlinear tracking method was tested. Momentary loss of signal or signal corruption does not affect the tracking process. The continuous nature of the algorithm presented here permits instantaneous tracking of the SCOLE attitude parameters regardless of the attitude time history.

System upgrading can contribute to error reduction. More powerful LEDs along with amplifier gain reduction will improve the signal-to-noise ratio. Improving sensor distortion mapping techniques will yield more accurate sensor output and, therefore, also more accurate attitude measurements.

VIII. REFERENCES

1. Taylor, L.W., Jr.; and Balakrishnan, A.V.: A Laboratory Experiment Used to Evaluate Control Laws for Flexible Spacecraft ... NASA/IEEE Design Challenge. Proceedings of the Fourth VPI&SU Symposium on Dynamics and Control of Large Structures, Blacksburg, VA, June 1983.
2. Williams, J.P.; and Rallo, R.A.: Description of the Spacecraft Control Laboratory Experiment (SCOLE) Facility. NASA TM-89057, January 1987.
3. Taylor, L.W. (Compiler): Spacecraft Control Laboratory Experiment, SCOLE Workshop -- Proceedings of a Workshop Concerning the NASA-IEEE Design Challenge. NASA Langley Research Center, Hampton, Virginia, December 6-7, 1984.
4. Taylor, L.W. (Compiler): 2nd Annual SCOLE Workshop -- Proceedings of a Workshop Concerning the NASA Design Challenge. NASA Langley Research Center, Hampton, Virginia, December 9-10, 1985. NASA TM-89048, October 1986.
5. Taylor, L.W. (Compiler): 3rd Annual SCOLE Workshop -- Proceedings of a Workshop Concerning the NASA Design Challenge. NASA Langley Research Center, Hampton, Virginia, November 17-18, 1986. NASA TM-89075, January 1987.

6. Taylor, L.W. (Compiler): 4th Annual SCOLE Workshop -- Proceedings of a Workshop Concerning the NASA Design Challenge. USAF Academy, Colorado Springs, Colorado, November 16, 1987. NASA TM-101503, October 1988.
7. Taylor, L.W. (Compiler): 5th Annual SCOLE Workshop -- Proceedings of a Workshop Concerning the NASA Design Challenge. Lake Arrowhead, California, October 31, 1988. NASA CP-10057 (Two Parts), December 1990.
8. Shenhar, J.; Sparks, D. Jr.; Williams, J.P.; and Montgomery, R.C.: Attitude Control System Testing on SCOLE. Proceedings of the Sixth VPI&SU/AIAA Symposium on Dynamics and Control of Large Flexible Spacecraft, June 28-July 1, 1987, Blacksburg, Virginia, pp. 251-273.
9. Montgomery, R.C.; Shenhar, J.; and Williams, J.P.: On-Line Identification and Attitude Control for SCOLE. Proceedings of the AIAA Guidance, Navigation and Control Conference, August 17-19, 1987, Monterey, California, pp. 950-958.
10. OP-EYE Optical Position Indicator. United Detector Technology, 12525 Chadron Avenue, Hawthorne, California.

11. Slama, C.C., (Editor-in-Chief): **Manual of Photogrammetry.**
American Society of Photogrammetry, Falls Church, Virginia, 4th
Edition, 1980.

12. Welch, S.S.; Montgomery, R.C.; and Barsky, M.F.: **The Spacecraft
Control Laboratory Experiment Optical Attitude Measurement
System.** NASA TM-102624, March 1991.

13. **PC-MATLAB for MS-DOS Personal Computers, Version 3.2-PC.** The
MathWorks, Inc., June 1987.

Table I.- Cameras orientation angles α , β , and ϵ
and scale factors λ

	α^0	β^0	ϵ^0	λ
CAMERA 1	89.58	-43.80	0.12	95.84
CAMERA 2	-87.58	-39.07	-1.52	102.54

ORIGINAL PAGE
BLACK AND WHITE PHOTOGRAPH

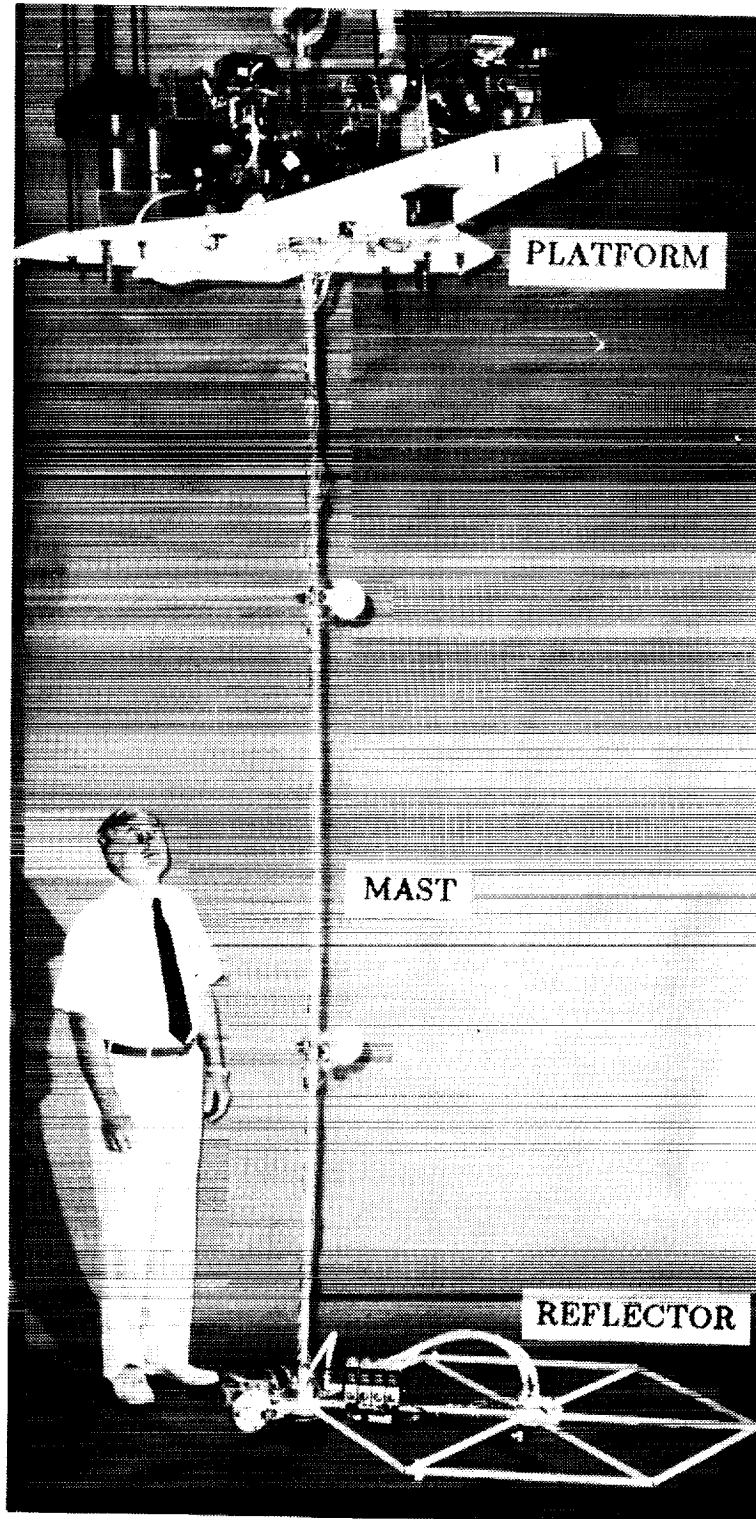


Figure 1.- The Spacecraft CONTROL Laboratory Experiment - SCOLE

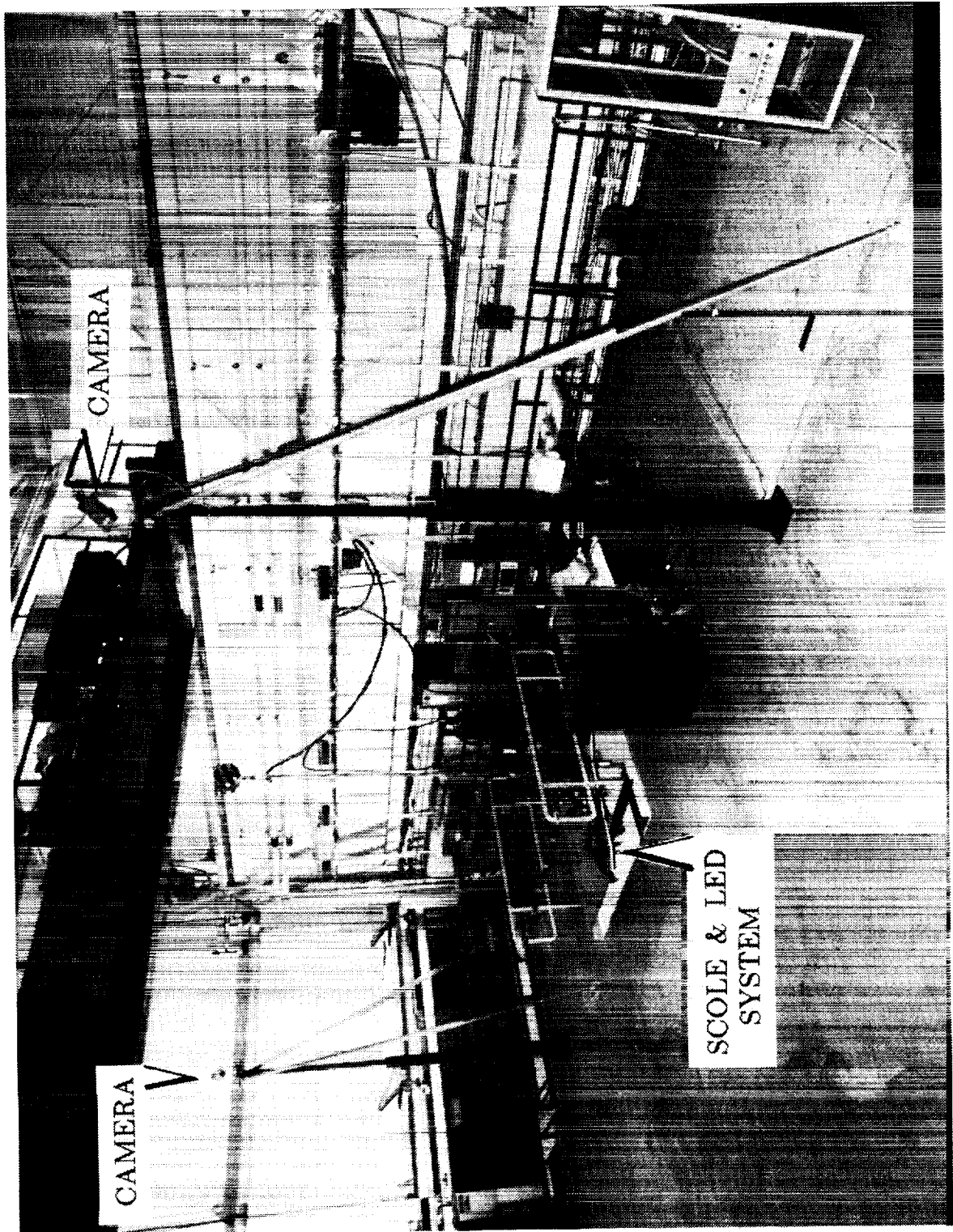


Figure 2.- SCOLE laboratory upper level view with two camera towers

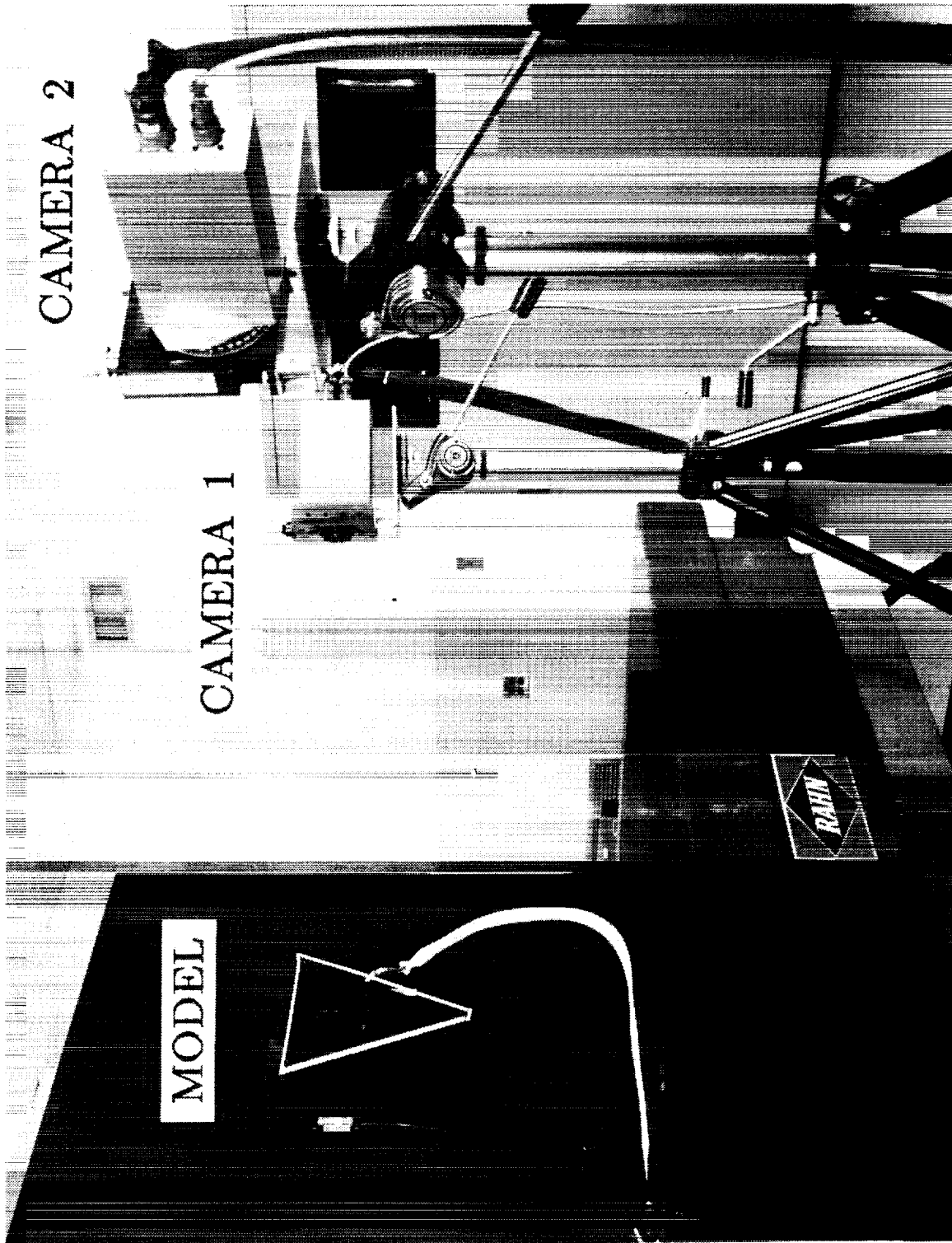


Figure 3.- Laboratory setup of infrared detector cameras and the SCOPE reduced-size model

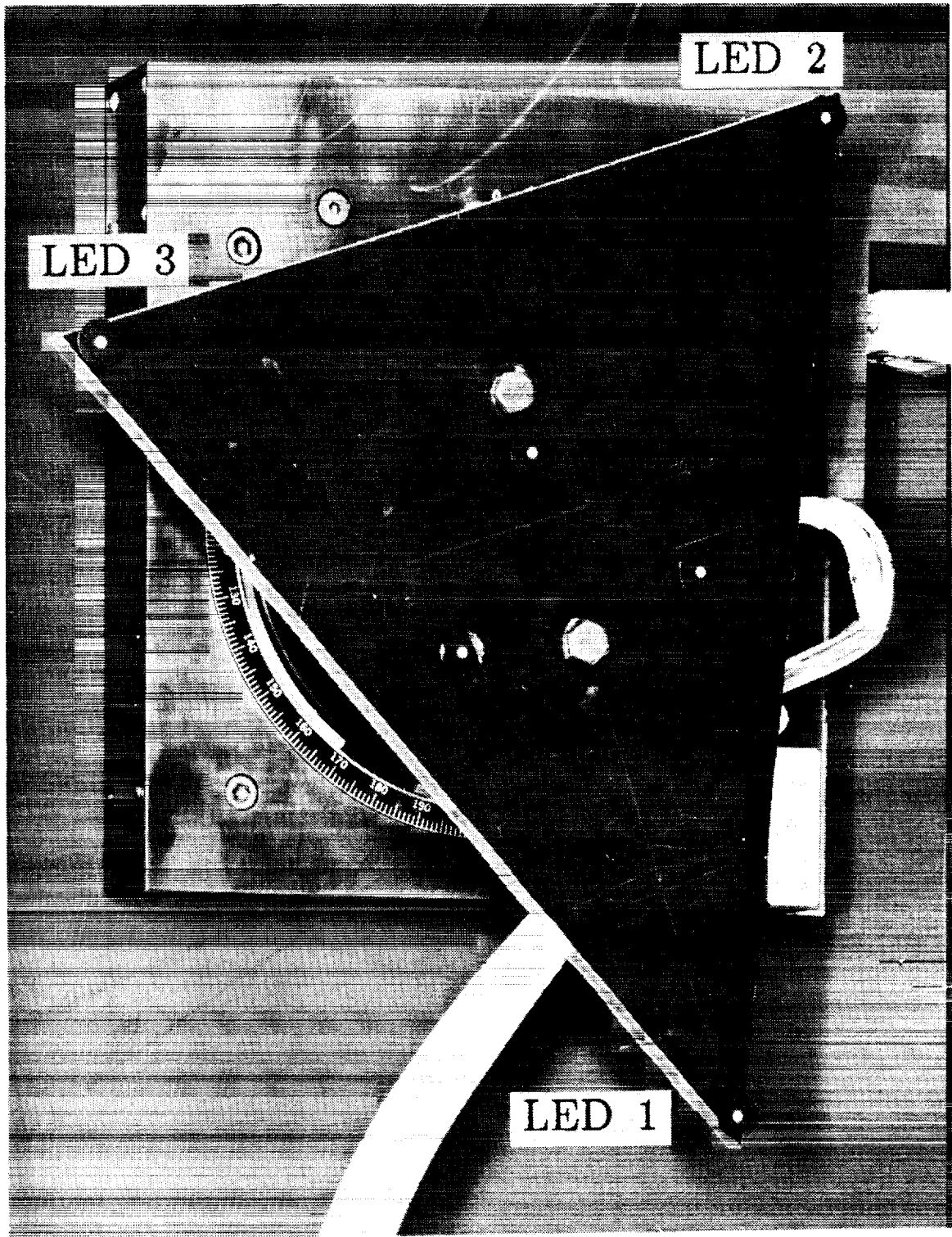


Figure 4.- SCOLE reduced-size model with LED configuration

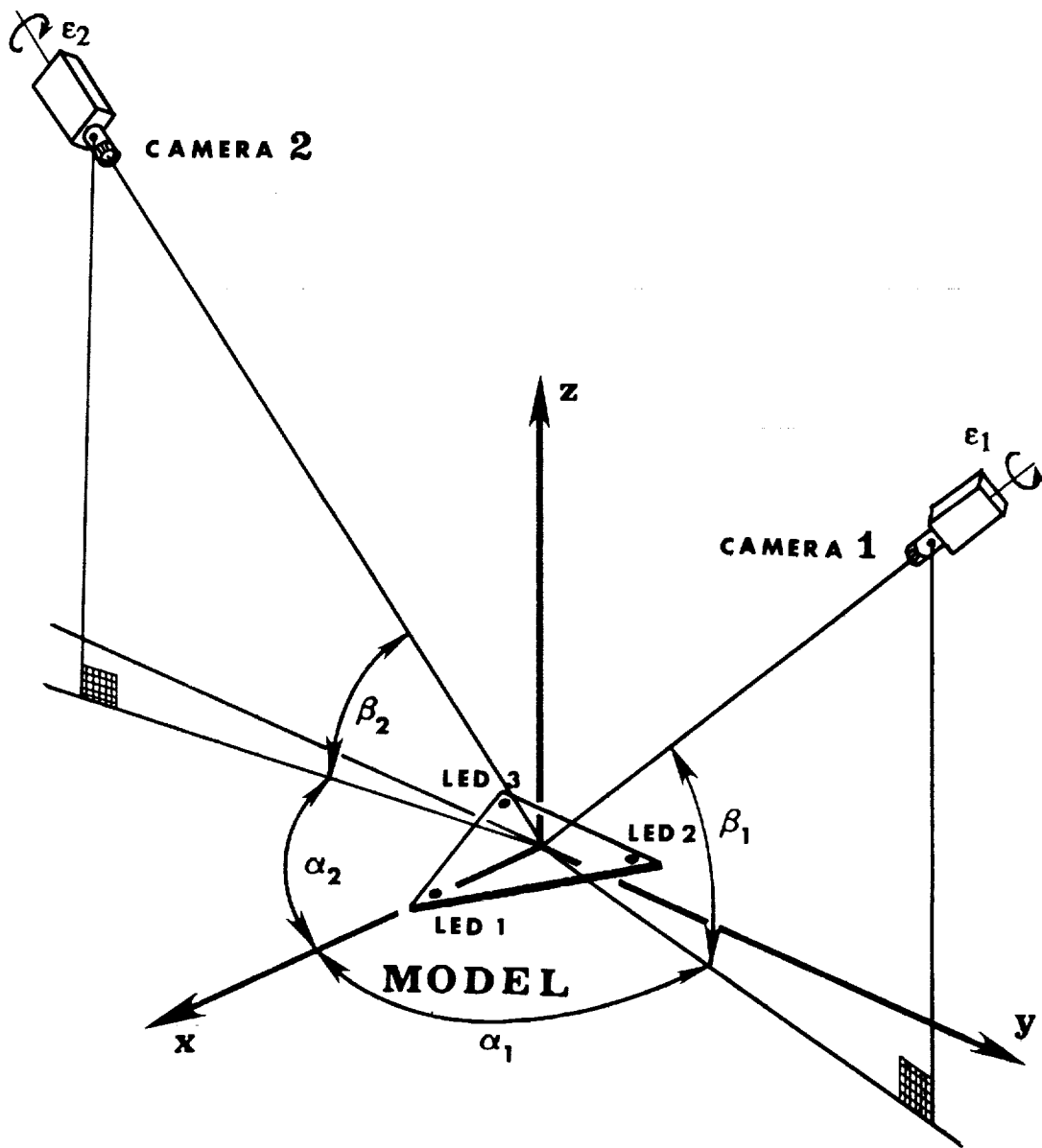


Figure 5 - Camera placement angles in Newtonian coordinates system

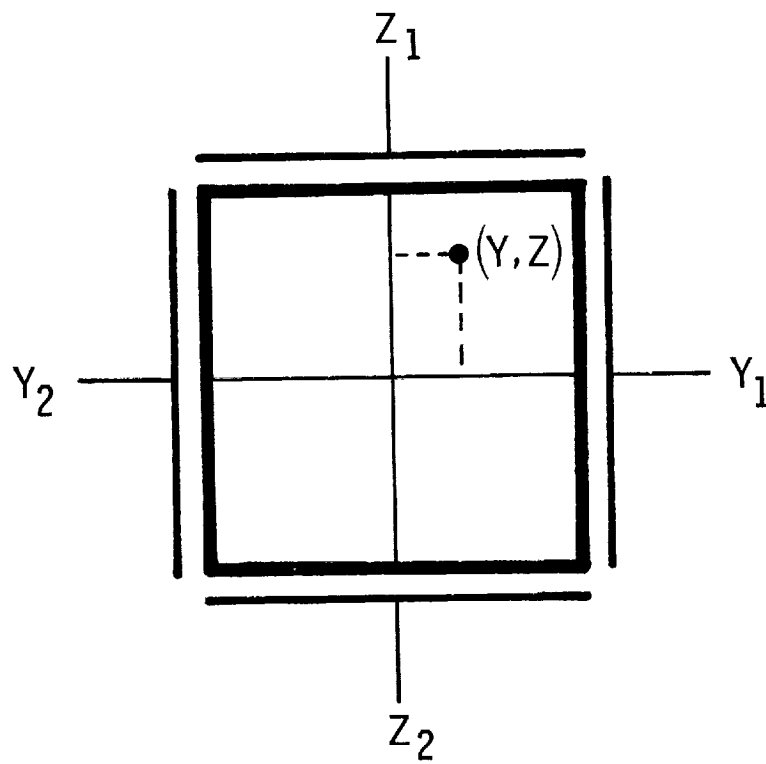


Figure 6 - True position (y,z) of a light spot on detector plane

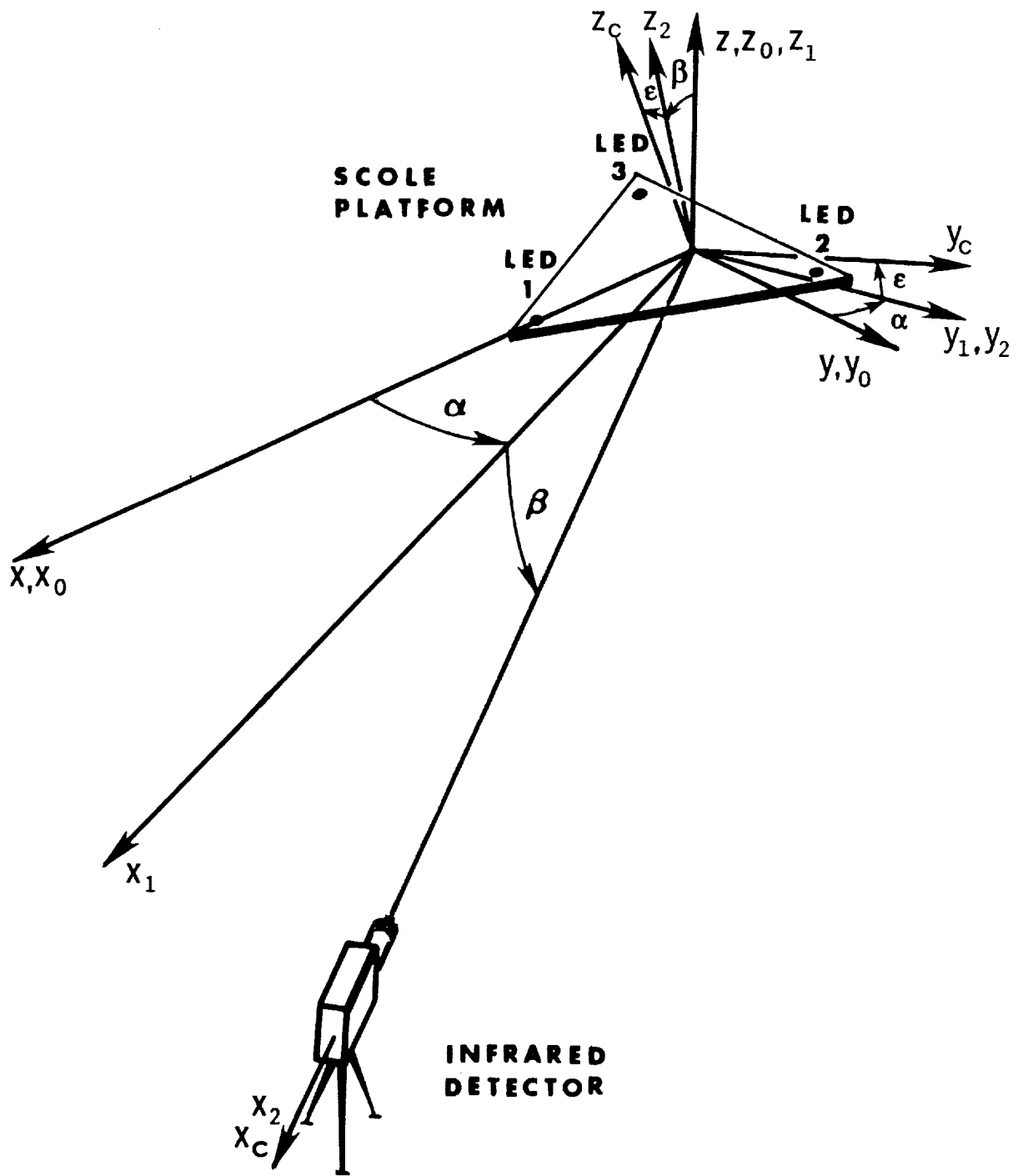


Figure 7.- Coordinate system transformation

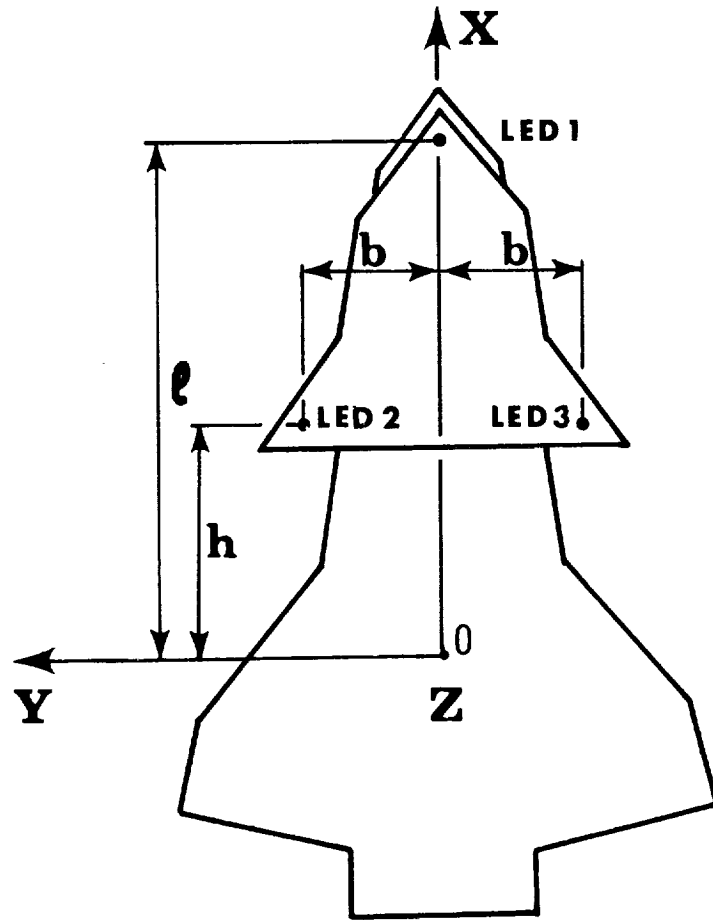


Figure 8 - LED placement configuration on SCOLE

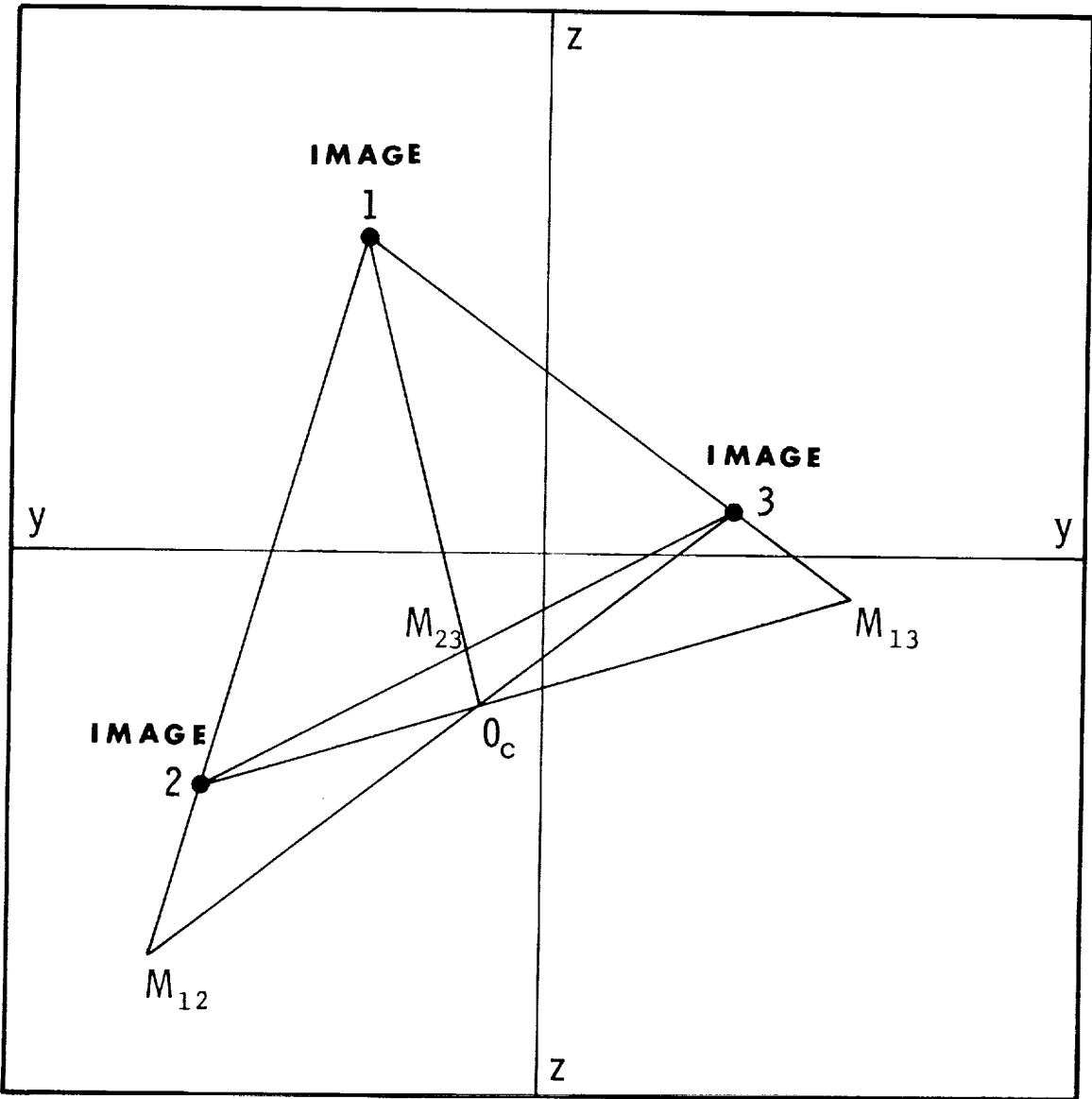


Figure 9.- LED image location and origin determination geometry on detector plane

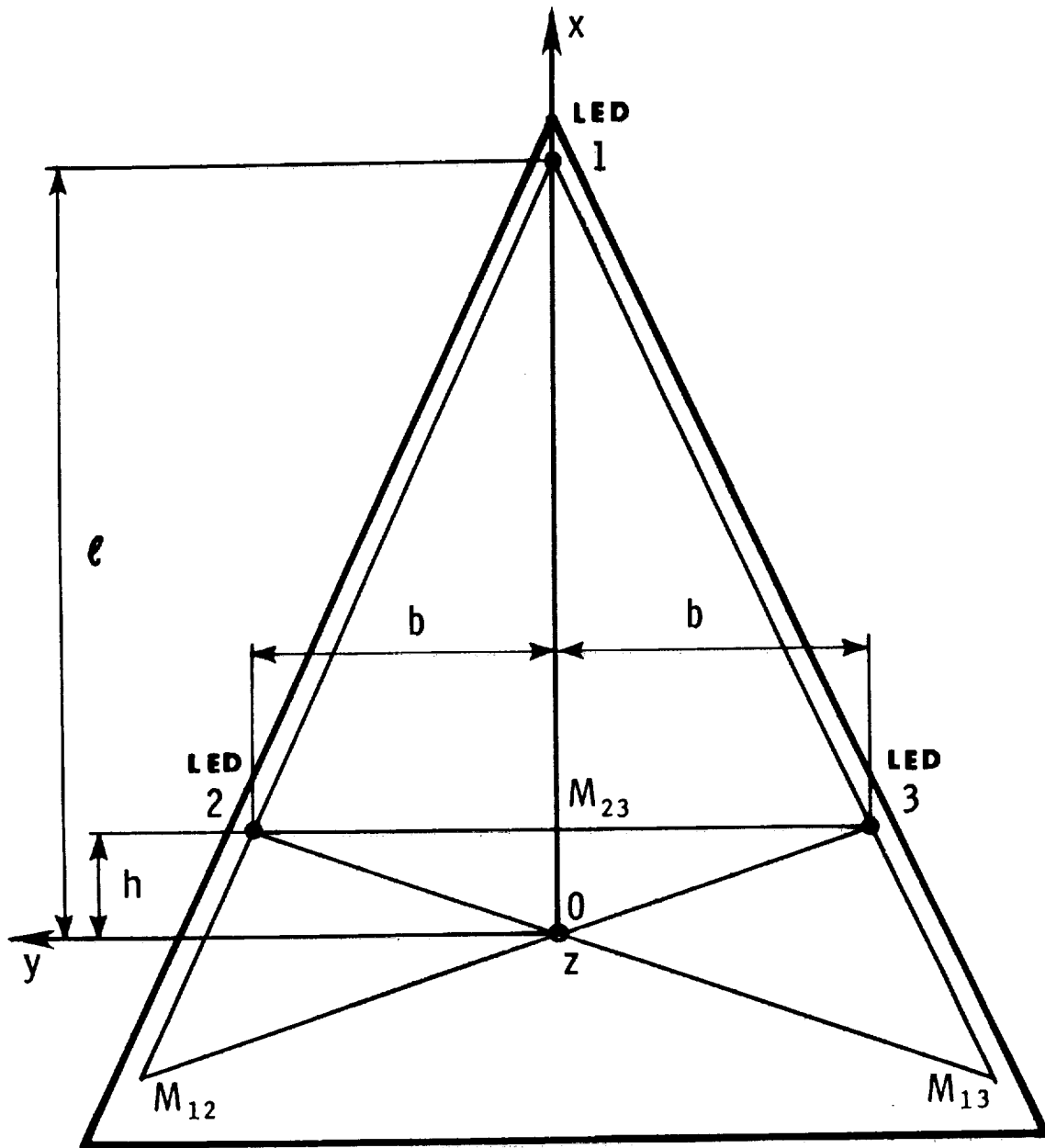


Figure 10.- LED triangular configuration on SCOLE

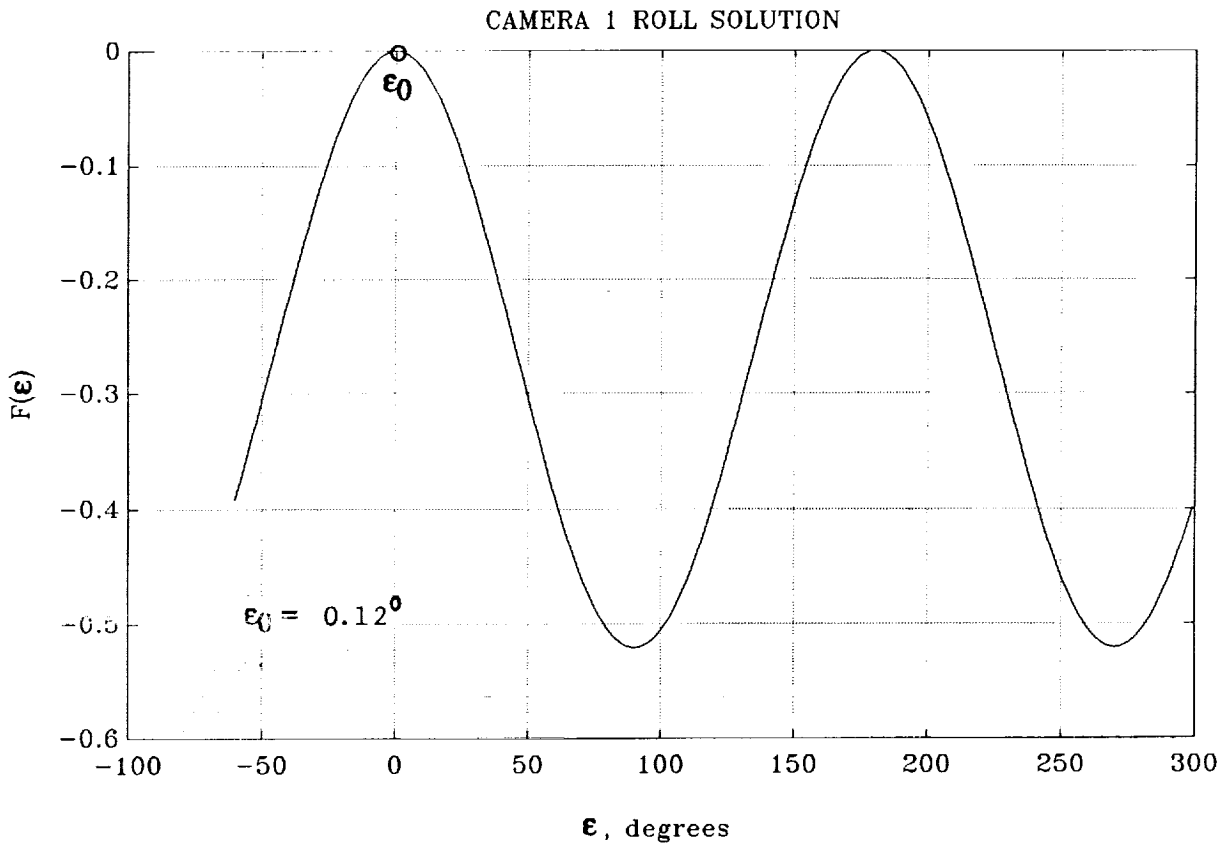


Figure 11.- A typical solution to Eq.(5): polynomial first root ϵ_0

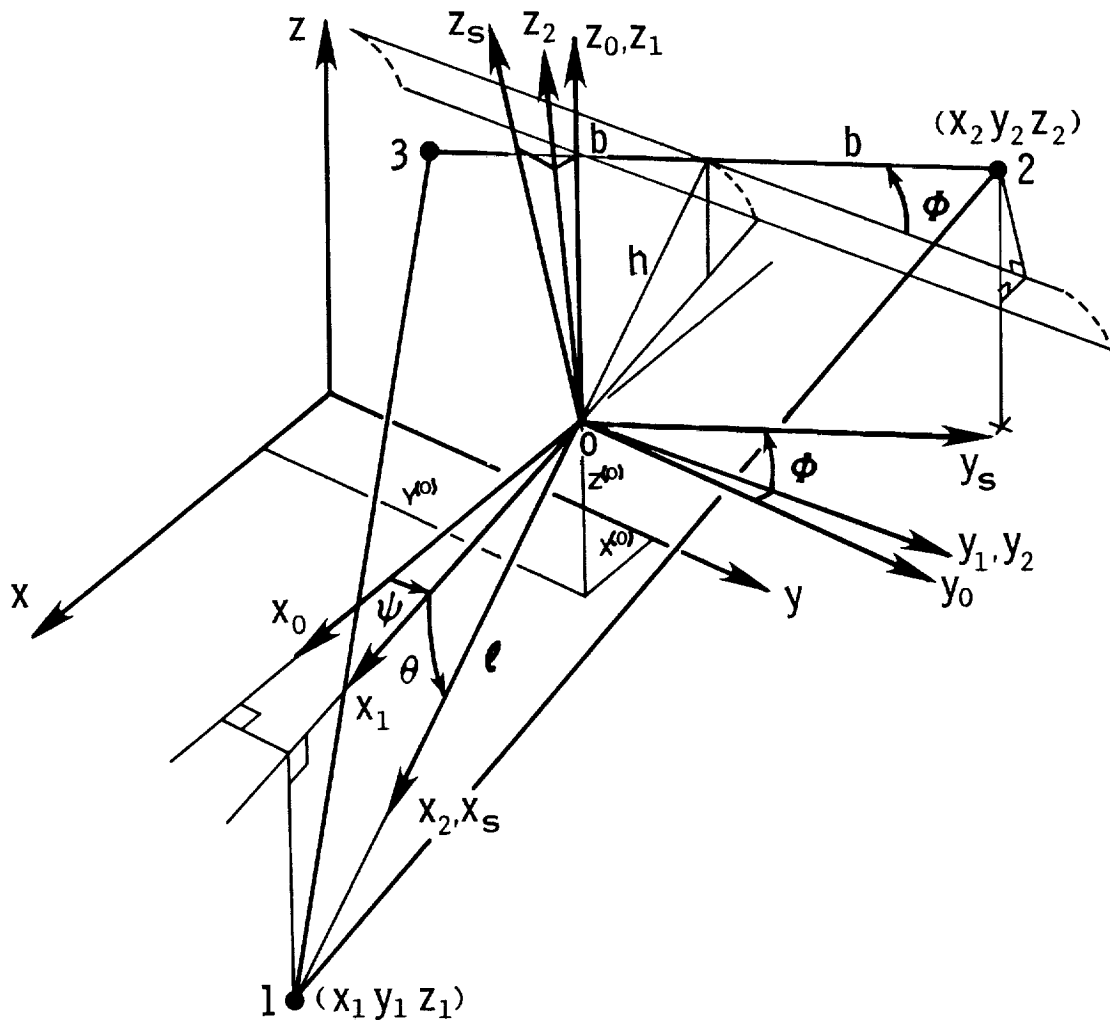
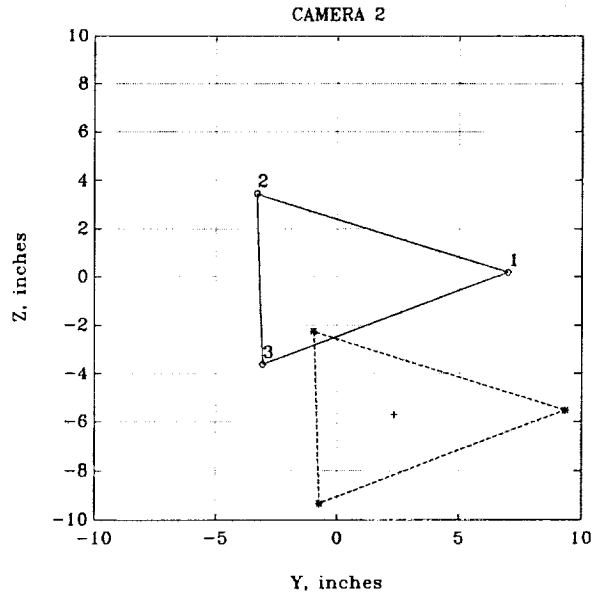
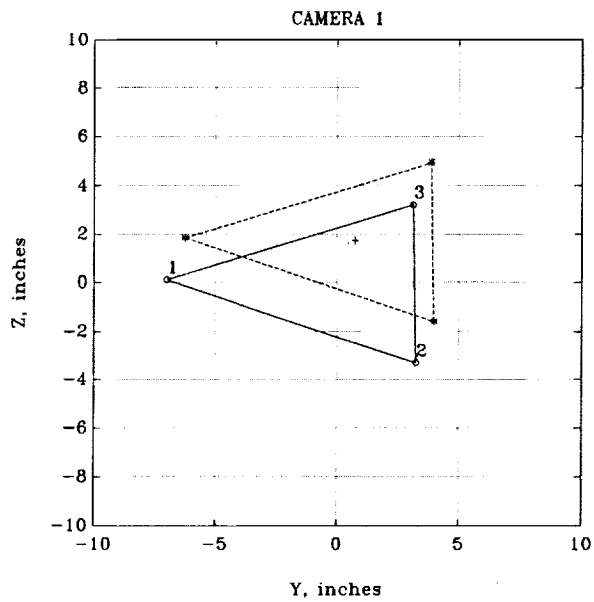


Figure 12.- SCOLE attitude angle extraction



- * Scaled LEDs absolute image
- + Scaled computed absolute image origin
- o Scaled LEDs relative image

Figure 13.- A typical scaled-image in the camera placement mode

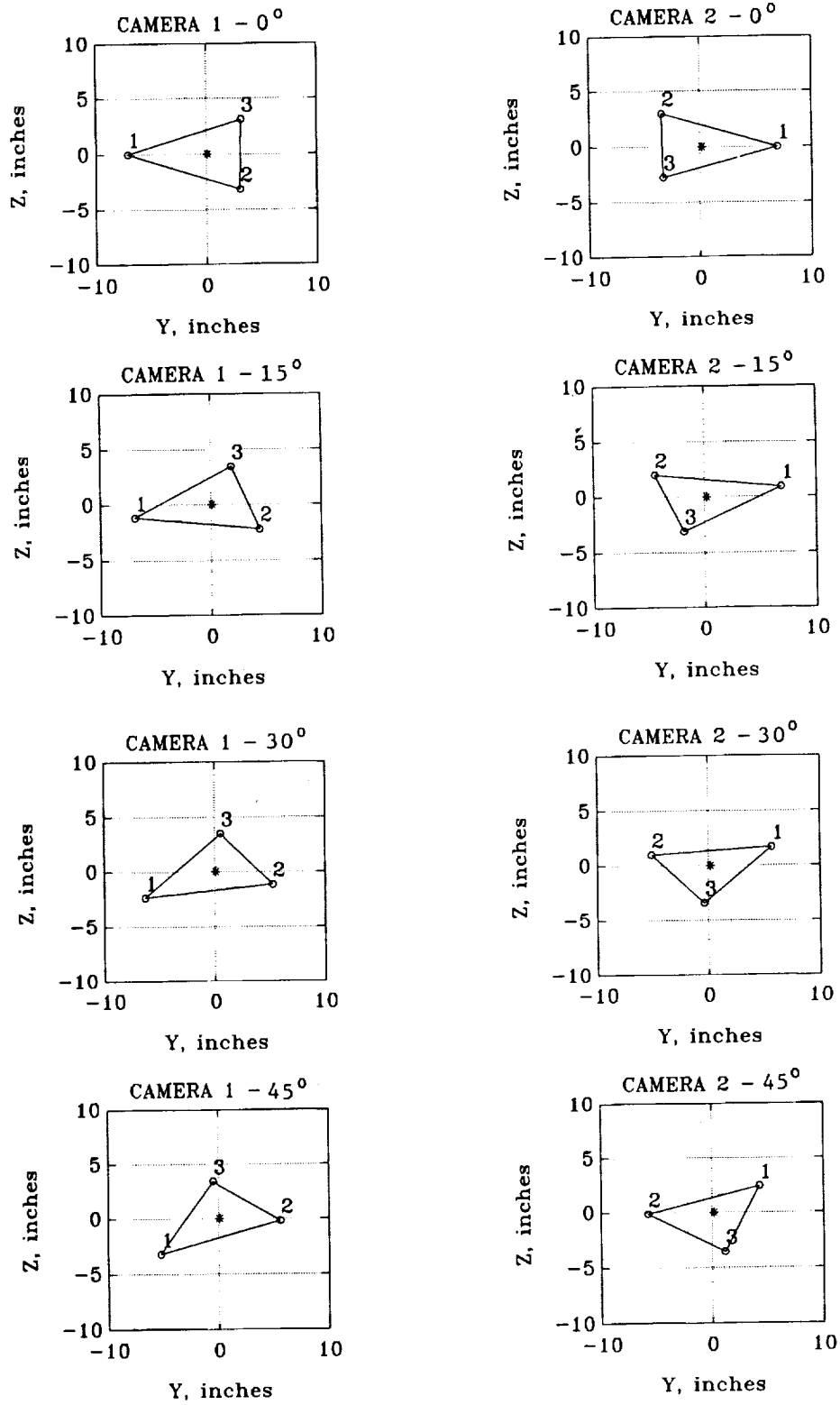


Figure 14.- Camera scaled-image at various model orientations

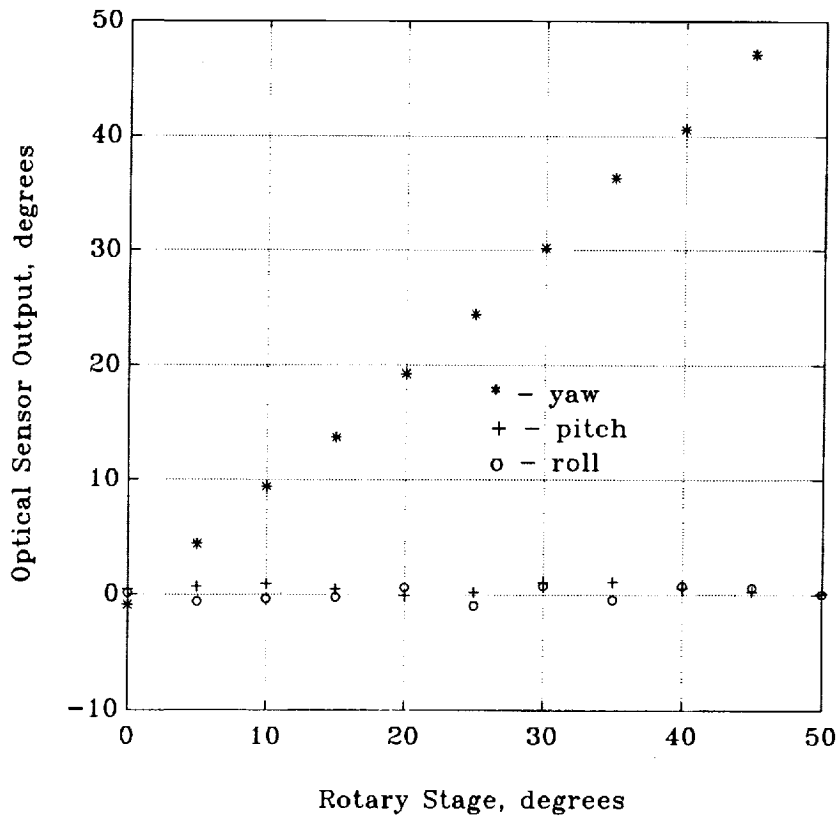


Figure 15.- Yaw, pitch, and roll measurements versus rotary stage position

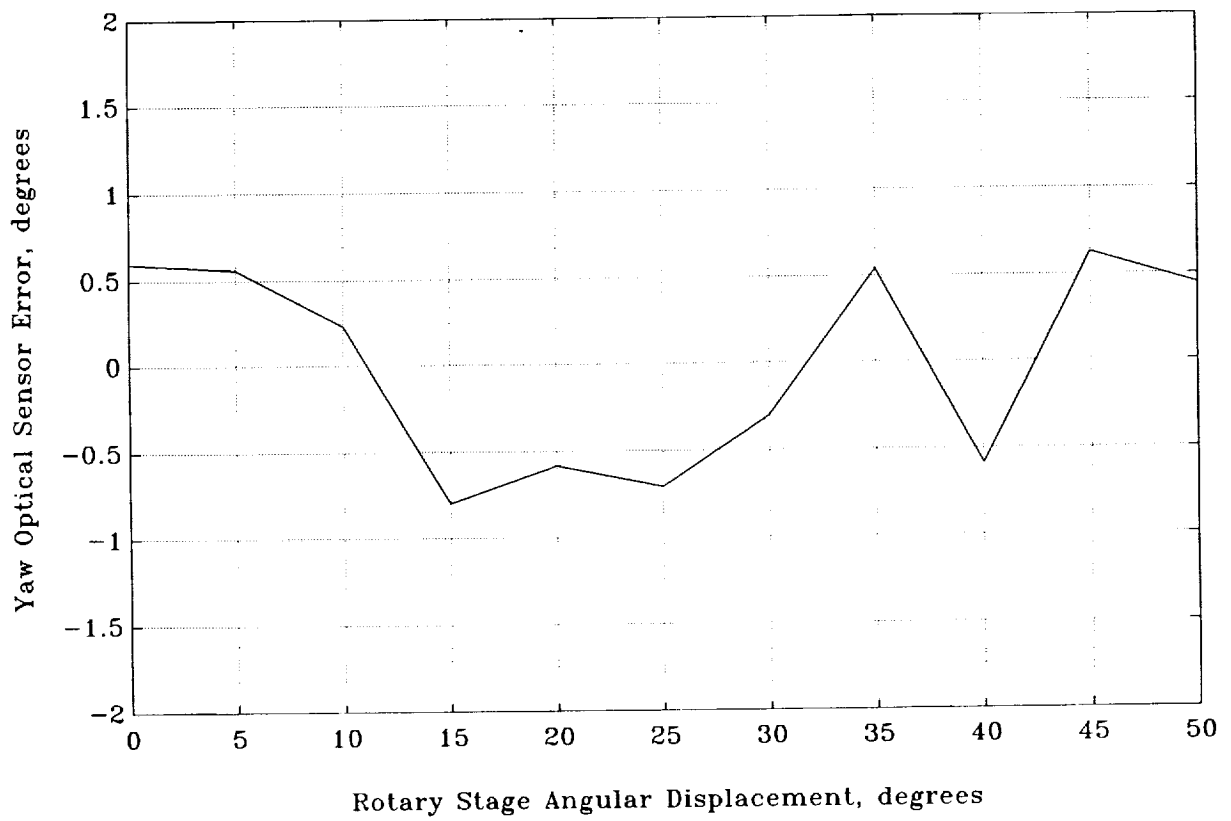


Figure 16.- Yaw attitude error via linear least-squares approximation

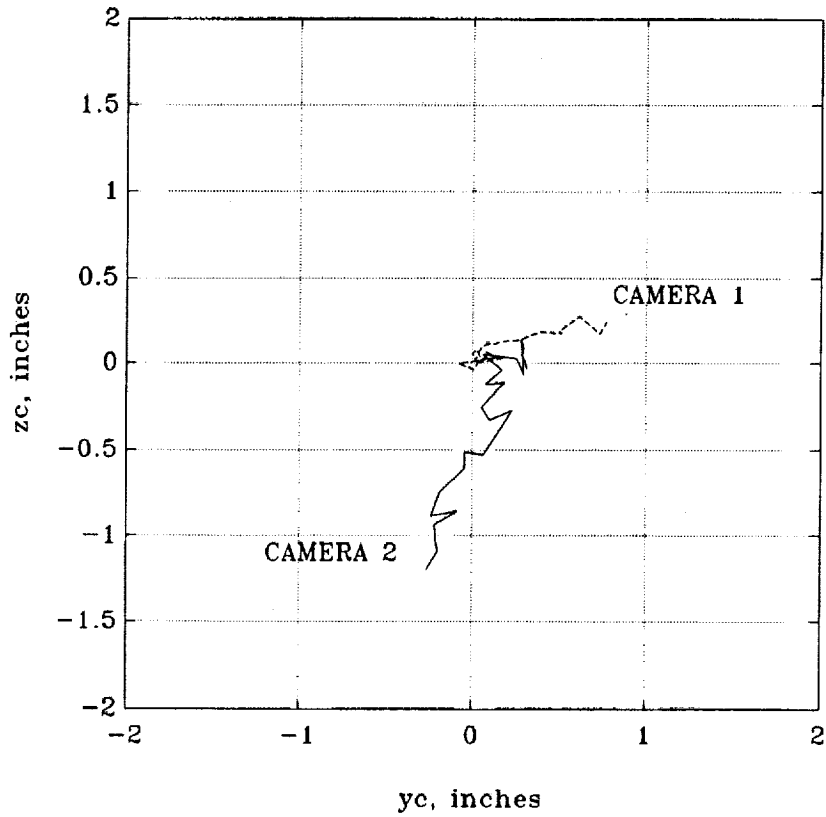


Figure 17.- Camera scaled view of center-of-mass motion

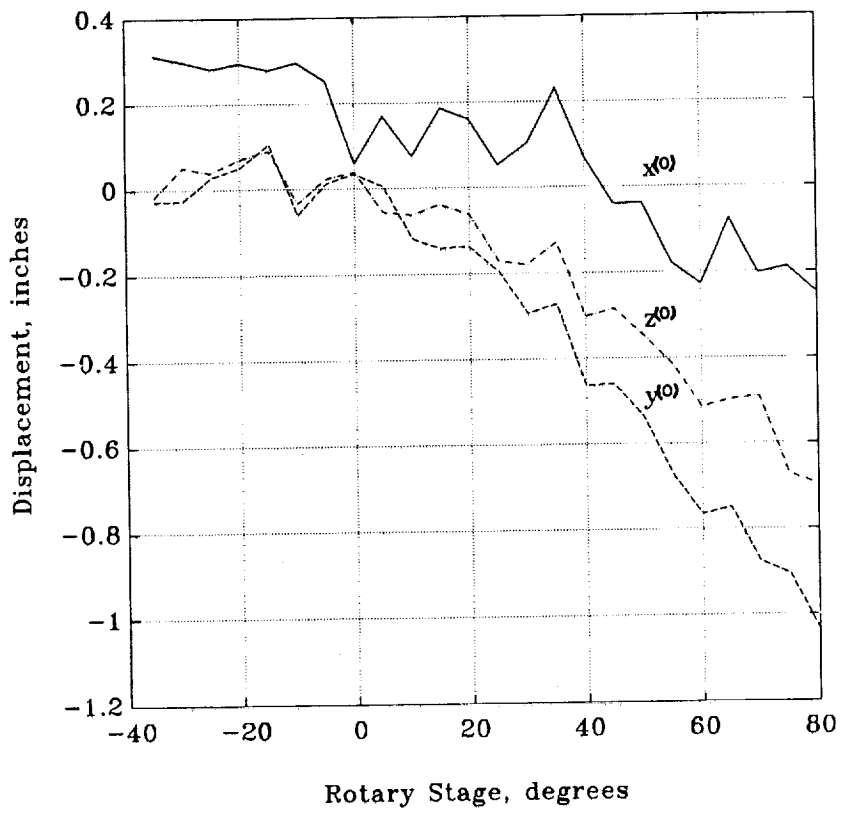


Figure 18.- $x(0)$, $y(0)$, $z(0)$ components of center-of-mass motion

APPENDIX

PC-MATLAB COMPUTER CODE FOR CAMERA PLACEMENT IDENTIFICATION AND SCOLE ATTITUDE TRACKING

PC-MATLAB computer language (ref.13) was used for the coding of the two-phase algorithm. The code consists of two main programs and thirteen sub-programs ".m" files. The first main program, "camid.m", provides a procedure for identification of the two camera attitude parameters with respect to a Newtonian frame. The second, "scolid.m", computes the instantaneous attitude parameters of the SCOLE platform with respect to that Newtonian frame. The sub-programs listed in the sequel, appear according to their first occurrence in the main calling program. The task of a program or a sub-program is explained under the NAME statement in each code.


```

eps1=xmax;
alpha1=alpha;
beta1=beta;
sf1=sf;
A1=A;B1=B;C1=C;
%
sf0=sf1;
rel % sub-program
cam=1;
relplot % sub-program
pause
%
% Determine CAM2 ABC coefficients
%
x100=x1;
y100=y1;
x1=x2;
y1=y2;
%
% Distortion corrector for CAM2
%
[x22,y22]=cammap2(x1,y1); % sub-program
x2=x22;
y2=y22;
x1=x100;
y1=y100;
sf20=50;
yc1=x2(1);
zc1=y2(1);
yc2=x2(2);
zc2=y2(2);
yc3=x2(3);
zc3=y2(3);
origin % sub-program
yc02=yc0;
zc02=zc0;
sf0=sf20;
rel % sub-program
abc % sub-program
scale % sub-program
cla
clg

```

```

eps2=xmax;
alpha2=alpha;
beta2=beta;
sf2=sf;
A2=A;B2=B;C2=C;
%
sf0=sf2;
rel                                     % sub-program
cam=2;
relplot                                  % sub-program
pause
%
!echo CAMERA 1 IDENTIFICATION
!echo *****
!echo .
sprintf('ALPHA-1    = %g',alpha1/dpr)
sprintf('BETA-1     = %g',beta1/dpr)
sprintf('EPSILON-1  = %g',eps1/dpr)
sprintf('SCALE FACTOR-1 = %g',sf1)
%
!echo .
!echo .
!echo CAMERA 2 IDENTIFICATION
!echo *****
!echo .
sprintf('ALPHA-2    = %g',alpha2/dpr)
sprintf('BETA-2     = %g',beta2/dpr)
sprintf('EPSILON-2  = %g',eps2/dpr)
sprintf('SCALE FACTOR-2 = %g',sf2)

```



```

y1=y11;
yc1=x1(1);
zc1=y1(1);
yc2=x1(2);
zc2=y1(2);
yc3=x1(3);
zc3=y1(3);
sf0=sf1;
yc0=yc01;
zc0=zc01;
rel                                     % sub-program
v1=[0 0 0
    yc10 yc20 yc30
    zc10 zc20 zc30];
%
% Distortion corrector for CAM2
%
x100=x1;
y100=y1;
x1=x2;
y1=y2;
[x22,y22]=cammap2(x1,y1);           % sub-program
x2=x22;
y2=y22;
x1=x100;
y1=y100;
yc1=x2(1);
zc1=y2(1);
yc2=x2(2);
zc2=y2(2);
yc3=x2(3);
zc3=y2(3);
sf0=sf2;
yc0=yc02;
zc0=zc02;
rel                                     % sub-program
v2=[0 0 0
    yc10 yc20 yc30
    zc10 zc20 zc30];
xcleat                                 % sub-program
v1(1,1:3)=v1(1,1:3)+xc(1,1:3);
v2(1,1:3)=v2(1,1:3)+xc(2,1:3);
vreal=INVR2*v2;

```

```

cla
sprintf('SCOLE CURRENT ATTITUDE:')
sprintf('*****')
angles                                     % sub-program

```

```

% NAME: flyy.m (sub-program)
% Routine activates the 8751 micro processor for
% camera data acquisition and storage in data arrays
%
function[x1,x2,y1,y2]=flyy()
data=camera(3);
for x=1:6;
    xa(x)=data((x-1)*8+1);
    xb(x)=data((x-1)*8+2);
    ya(x)=data((x-1)*8+3);
    yb(x)=data((x-1)*8+4);
    xa2(x)=data((x-1)*8+5);
    xb2(x)=data((x-1)*8+6);
    ya2(x)=data((x-1)*8+7);
    yb2(x)=data((x-1)*8+8);
end;
x1=(xa-xb)./(xa+xb);%-.14187;
x2=(xa2-xb2)./(xa2+xb2);%+.0702;
y1=(ya-yb)./(ya+yb);%+.0287;
y2=(ya2-yb2)./(ya2+yb2);%-.07604;

```

```

% NAME: scolpar.m (sub-program)
% SCOLE's Hardware parameters input
%
l=7.0;
h=(3+3/16);
b=4.5;
v0=[l -h -h
    0 b -b
    0 0 0];
%
dpr=pi/180;

```

```

% NAME:  preorigin.m (sub-program)
% Routine computes parameters related to the
%   LEDs placement geometry
%
% Subscript "s" means SCOLE, "c" means CAMERA
%
% Coordinates on SCOLE:
%
xs1=v0(1,1);
ys1=v0(2,1);
zs1=v0(3,1);
xs2=v0(1,2);
ys2=v0(2,2);
zs2=v0(3,2);
xs3=v0(1,3);
ys3=v0(2,3);
zs3=v0(3,3);
%
% SCOLE platform triangular geometry
%
% M12 coordinates:
%
xs12=-xs1*xs2/(xs1-2*xs2);
ys12=ys2*xs1/(xs1-2*xs2);
%
% M23 coordinates:
%
xs23=xs2;
ys23=0;
bar1M12=sqrt((xs1-xs12)^2+(ys1-ys12)^2);
bar12=sqrt((xs1-xs2)^2+(ys1-ys2)^2);
ratio12=bar1M12/bar12;
ratio23=0.5;

```

```

% NAME:  cammap1.m (sub-program)
% CAM1 detector map for distortion correction
%
function [x11,y11]=cammap1(x1,y1)
for x=1:6;
    xp(x)=-.0137+.1702*x1(x)-.0003*y1(x)+.0018*(x1(x)*y1(x));
    xpp(x)=xp(x)-.0113*x1(x)^2-.0052*y1(x)^2;

```

```

x1p(x)=xpp(x)-.0019*x1(x)^2*y1(x)+.0212*x1(x)*y1(x)^2;
x1l(x)=x1p(x)+.0884*x1(x)^3-.0036*y1(x)^3;
yp(x)=.0035-.0006*x1(x)+.1721*y1(x)-.0019*x1(x)*y1(x);
ypp(x)=yp(x)+.0085*x1(x)^2+.0006*y1(x)^2;
y1p(x)=ypp(x)+.0423*x1(x)^2*y1(x)-.003*x1(x)*y1(x)^2;
y1l(x)=y1p(x)+.0107*x1(x)^3+.0678*y1(x)^3;
end;

```

```

% NAME:  origin.m (sub-program)
% Routine computes the coordinates of SCOLE's origin
%   in the camera frame.
%
% CAMERA frame triangular geometry
%
yc12=yc1+(yc2-yc1)*ratio12;
zc12=zc1+(zc2-zc1)*ratio12;
yc23=yc2+(yc3-yc2)*ratio23;
zc23=zc2+(zc3-zc2)*ratio23;
%
% Equation of line 3-M12
%
m12=(zc3-zc12)/(yc3-yc12);
b12=(yc3*zc12-zc3*yc12)/(yc3-yc12);
%
% Equation of line 1-M23
%
m23=(zc1-zc23)/(yc1-yc23);
b23=(yc1*zc23-zc1*yc23)/(yc1-yc23);
%
% Coordinates of origin in camera's frame
%
zc0=(m12*b23-m23*b12)/(m12-m23);
yc0=-(b12-b23)/(m12-m23);

```

```

% NAME:  rel.m (sub-program)
% Routine computes the projections of the position
% vectors of SCOLE's LEDs
%
yc10=(yc1-yc0)*sf0;
zc10=(zc1-zc0)*sf0;
yc20=(yc2-yc0)*sf0;
zc20=(zc2-zc0)*sf0;
yc30=(yc3-yc0)*sf0;
zc30=(zc3-zc0)*sf0;

```

```

% NAME:  abc.m (sub_program)
% Routine computes the polynomial coefficients of equation (5a).
%
A=((yc20+yc30)/2/h)^2+((yc20-yc30)/2/b)^2;
B=(yc20+yc30)*(zc20+zc30)/2/h/h+(yc20-yc30)*(zc20-zc30)/2/b/b;
C=((zc20+zc30)/2/h)^2+((zc20-zc30)/2/b)^2;

```

```

% FILE NAME:  scale.m (sub-program)
% Routine computes camera scale factor and the
% camera placement parameters, the angles ALPHA, BETA,
% and EPSILON
%
dpr=pi/180;
A0=A;B0=B;C0=C;
maxold=0;
delta=1;
i0=31;
ifin=61;
xbegin=0;
convrg=0.0000001;
convdel=0.001; %degrees
flag=0;
sf=sf0;
for j=1:1000
%
clear xx yy
for i=1:ifin
x=xbegin+(i-i0)*delta;

```

```

    xx(i)=x;
    x=x*dpr;
    yy(i)=A*(cos(x))^2-B*sin(x)*cos(x)+C*(sin(x))^2-1;
    x=x/dpr;
end
%
    [maxyy,ii]=max(yy);
    xmax=xx(ii);
%
    xbegin=xmax-2*delta;
    delta=delta/2;
    i0=0;
    ifin=8;
    if delta<=convdel&abs(maxyy)<=convrg
        break
    end
%
    maxold=maxyy;
    sf=sf*sqrt(1/(1+maxyy));
    sfr=sf/sf0;
    sfrsq=sfr^2;
    A=A0*sfrsq; B=B0*sfrsq; C=C0*sfrsq;
end
%
s1=(yc20+yc30)/2/h*(-sign(v0(1,2)));
s2=(zc20+zc30)/2/n*(-sign(v0(1,2)));
c1=(yc20-yc30)/2/b;
c2=(zc20-zc30)/2/b;
s1=s1*sfr;s2=s2*sfr;c1=c1*sfr;c2=c2*sfr;
xmax=xmax*dpr;
%
alpha=(asin(s1*cos(xmax)-s2*sin(xmax)));
beta=asin((c2+sin(xmax)*cos(alpha))/cos(xmax)/sin(alpha));

% NAME: relplot.m (sub-program)
% Routine plots the relative coordinates of the LEDs
% image on the detector plane
%
yyrel=[yc10 yc20 yc30];
zzrel=[zc10 zc20 zc30];
yy=[yc1 yc2 yc3];

```

```

zz=[zc1 zc2 zc3];
axis('square')
axis([-8,8,-8,8])
plot(yyrel,zzrel,'o')
hold
%
yy=yy*sf0;
zz=zz*sf0;
yc0=yc0*sf0;
zc0=zc0*sf0;
%
plot(yy,zz,'+',yc0,zc0, '*')
num=['1' '2' '3'];
setstr(num)
for i=1:3
    text(yyrel(i),zzrel(i),num(i))
end
if (cam==1);title('CAMERA 1 ACTUAL DATA');end
if (cam==2);title('CAMERA 2 ACTUAL DATA');end
grid
hold off

```

```

% NAME: cammap2.m
% CAM2 detector map for distortion correction
%
function [x11,y11]=cammap2(x1,y1)
for x=1:6;
    xp(x)=.0215+.1463*x1(x)-.0051*y1(x)-.0021*(x1(x)*y1(x));
    xpp(x)=xp(x)+.0017*x1(x)^2+.0133*y1(x)^2;
    x1p(x)=xpp(x)-.0005*x1(x)^2*y1(x)+.0074*x1(x)*y1(x)^2;
    x11(x)=x1p(x)+.076*x1(x)^3-.0074*y1(x)^3;
    yp(x)=-.0193+.0027*x1(x)+.1881*y1(x)+.0033*x1(x)*y1(x);
    ypp(x)=yp(x)-.0166*x1(x)^2+.0066*y1(x)^2;
    y1p(x)=ypp(x)+.0327*x1(x)^2*y1(x)-.0088*x1(x)*y1(x)^2;
    y11(x)=y1p(x)+.0024*x1(x)^3+.0711*y1(x)^3;
end;

```

```

% NAME:  tmatrix.m (sub-program)
% Routine computes the R=EPS*BETA*ALPHA
%   transformation matrix
%
salpha=sin(alpha);
calpha=cos(alpha);
sbeta=sin(beta);
cbeta=cos(beta);
seps=sin(eps);
ceps=cos(eps);
ALPHA=[calpha salpha 0;-salpha calpha 0;0 0 1];
BETA=[cbeta 0 -sbeta;0 1 0; sbeta 0 cbeta];
EPS=[1 0 0;0 ceps seps;0 -seps ceps];
R=EPS*BETA*ALPHA;

```

```

% NAME:  xcleast.m (sub-program)
% Routine computes the xc1, xc2 components via
%   least squares approximation
%
D=[1 -R(1,1)
   0 -R(2,1)
   0 -R(3,1)];
DTR=D';
F=inv(DTR*D);
E=[R(1,2) R(1,3)
   R(2,2) R(2,3)
   R(3,2) R(3,3)];
subv2=v2(2:3,1:3);
subv1=[0      0      0
       v1(2,1) v1(2,2) v1(2,3)
       v1(3,1) v1(3,2) v1(3,3)];
xc=F*DTR*(E*subv2-subv1);

```

```

% FILE NAME:  angles.m (sub-program)
% routine computes the attitude parameters based upon
%   the (xi,yi,zi), i=1,2,3 coordinates
%
x=vreal(1,1:3);
y=vreal(2,1:3);

```

```

z=vreal(3,1:3);
%
% Compute the attitude angles PSI,THETA, FI
%
psi=atan(y(1)/x(1));
theta=atan(-z(1)/sqrt(x(1)^2+y(1)^2));
hh=h*(-sign(v0(1,2)));
xbar=x(2)+hh*cos(theta)*cos(psi);
ybar=y(2)+hh*cos(theta)*sin(psi);
zbar=z(2)-hh*sin(theta);
b1=sqrt(xbar^2+ybar^2+zbar^2);
phi=asin((z(2)-hh*sin(theta))/cos(theta)/b1);
sprintf('YAW.....PSI (degrees) = %g',psi/dpr)
sprintf('PITCH.....THETA (degrees) = %g',theta/dpr)
sprintf('ROLL.....PHI (degrees) = %g',phi/dpr)

```



Report Documentation Page

1. Report No. NASA CR-4397	2. Government Accession No.	3. Recipient's Catalog No.	
4. Title and Subtitle Attitude Identification for SCOLE Using Two Infrared Cameras		5. Report Date October 1991	6. Performing Organization Code
		8. Performing Organization Report No.	
7. Author(s) Joram Shenhar		10. Work Unit No. 506-59-61-01	
9. Performing Organization Name and Address Lockheed Engineering & Sciences Co. 144 Research Drive Hampton, VA 23666		11. Contract or Grant No. NAS1-19000	
		13. Type of Report and Period Covered Contractor Report Interim Report	
12. Sponsoring Agency Name and Address National Aeronautics and Space Administration Langley Research Center Hampton, VA 23665-5225		14. Sponsoring Agency Code	
		15. Supplementary Notes Langley Technical Monitor: Raymond C. Montgomery	
16. Abstract <p>This report presents an algorithm that incorporates real-time data from two infrared cameras and computes the attitude parameters of the Spacecraft Control Laboratory Experiment (SCOLE), a laboratory apparatus representing an offset-feed antenna attached to the Space Shuttle by a flexible mast. The algorithm utilizes camera position information of three miniature light emitting diodes (LEDs), mounted on the SCOLE platform, permitting arbitrary camera placement and an on-line attitude extraction. The continuous nature of the algorithm allows identification of the placement of the two cameras with respect to some initial position of the three reference LEDs, followed by on-line six degrees of freedom attitude tracking, regardless of the attitude time history. The report provides a description of the algorithm in the camera identification mode as well as the mode of target tracking. Experimental data from a reduced-size SCOLE-like laboratory model, reflecting the performance of the camera identification and the tracking processes, are presented. Computer code for camera placement identification and SCOLE attitude tracking is listed.</p>			
17. Key Words (Suggested by Author(s)) Attitude Tracking Arbitrary Camera Placement Least Squares Approximation		18. Distribution Statement Unclassified-Unlimited Subject Category 35	
19. Security Classif. (of this report) Unclassified	20. Security Classif. (of this page) Unclassified	21. No. of pages 68	22. Price A04